AFRL-RH-WP-TR-2009-0041

Modeling of Complex Mixtures: JP-8 Toxicokinetics

Teresa R. Sterner
Peter J. Robinson
Elaine A. Merrill
Michael J. Wagner
David R. Mattie

Applied Biotechnology Branch
2729 R Street
Wright-Patterson AFB OH 45433-5707

October 2008

Final Report for October 2005 – September 2008

Air Force Research Laboratory
711th Human Performance Wing
Human Effectiveness Directorate
Biosciences and Protection Division
Applied Biotechnology Branch
Wright-Patterson AFB OH 45433-5707

NOTICE

Using Government drawings, specifications, or other data included in this document for any purpose other than Government procurement does not in any way obligate the U.S. Government. The fact that the Government formulated or supplied the drawings, specifications, or other data does not license the holder or any other person or corporation; or convey any rights or permission to manufacture, use, or sell any patented invention that may relate to them.

This report was cleared for public release by the 88th Air Base Wing Public Affairs Office and is available to the general public, including foreign nationals. Copies may be obtained from the Defense Technical Information Center (DTIC) (http://www.dtic.mil).

AFRL-RH-WP-TR-2009-0041

THIS REPORT HAS BEEN REVIEWED AND IS APPROVED FOR PUBLICATION IN
ACCORDANCE WITH ASSIGNED DISTRIBUTION STATEMENT.

This report is published in the interest of scientific and technical information exchange, and its publication does not constitute the Government's approval or disapproval of its ideas or findings.

REPORT DOCUMENTATION PAGE

1. REPORT DATE *(DD-MM-YYYY)* October 2008	2. REPORT TYPE Final	3. DATES COVERED *(From - To)* 1-Oct-05 – 30-Sep-08

4. TITLE AND SUBTITLE Modeling of Complex Mixtures: JP-8 Toxicokinetics	5a. CONTRACT NUMBER
	5b. GRANT NUMBER NA
	5c. PROGRAM ELEMENT NUMBER 62202F

6. AUTHOR(S) Teresa R. Sterner, Peter J. Robinson, Elaine A. Merrill, Michael J. Wagner, David R. Mattie	5d. PROJECT NUMBER 2312
	5e. TASK NUMBER A2
	5f. WORK UNIT NUMBER 2312A215

7. PERFORMING ORGANIZATION NAME(S) AND ADDRESS(ES) 711 HPW/RHPB 2729 R Street Wright-Patterson AFB OH 45433-5707	8. PERFORMING ORGANIZATION REPORT NUMBER

9. SPONSORING / MONITORING AGENCY NAME(S) AND ADDRESS(ES) Air Force Materiel Command Air Force Research Laboratory 711th Human Performance Wing Human Effectiveness Directorate Biosciences and Protection Division Applied Biotechnology Branch Wright-Patterson AFB OH 45433-5707	10. SPONSOR/MONITOR'S ACRONYM(S) 711 HPW/RHPB
	11. SPONSOR/MONITOR'S REPORT NUMBER(S) AFRL-RH-WP-TR-2009-0041

12. DISTRIBUTION / AVAILABILITY STATEMENT

Approved for public release; distribution unlimited.

13. SUPPLEMENTARY NOTES
Cleared by 88 ABW/PA 19 May 09, Case Number 88ABW-2009-2091.

14. ABSTRACT
This report culminates a three year project to develop appropriately parameterized and validated physiologically-based pharmacokinetic (PBPK) models for representative components of jet fuel JP-8, and combine them into a complex mixture interaction model of JP-8 itself for use in a mechanism-based assessment of human health effects resulting from exposure to aerosol, vapor and (via skin) liquid. Single chemical models of selected representative components (nonane, decane and naphthalene) were used to predict systemic dose for dose-response assessment using kinetic data from in-house and published studies. To harmonize single chemical models, we developed a modeling framework that included generic tissue compartments in which we have combined diffusion limitation and deep tissue (global tissue model). We also applied a QSAR approach for estimating blood and tissue partition coefficients, and in integrating our kinetic model with exposure models. A complex mixture model of jet fuel was developed for an arbitrarily large number of components, in which interactions are modeled for the specific case of competitive metabolic inhibition of a specific enzyme (P450-2E1). Applications of this approach include the ability to integrate animal, human and *in vitro* data in a form that allows internal dose and health effects predictions to be made concerning specific real-world exposures to JP-8 and new alternative fuels.

15. SUBJECT TERMS
jet fuel, JP-8, PBPK modeling, complex mixtures, nonane, decane, naphthalene, QSAR, alternative fuels

16. SECURITY CLASSIFICATION OF:			17. LIMITATION OF ABSTRACT	18. NUMBER OF PAGES	19a. NAME OF RESPONSIBLE PERSON David R. Mattie
a. REPORT U	b. ABSTRACT U	c. THIS PAGE U	SAR	59	19b. TELEPHONE NUMBER *(include area code)* NA

THIS PAGE INTENTIONALLY LEFT BLANK.

TABLE OF CONTENTS

LIST OF FIGURES

LIST OF TABLES

PREFACE

SUMMARY

The overall context of our work is shown in Figure 1. Single chemical studies of individual components, such as nonane, decane and naphthalene, and complex mixture models are used to predict a systemic dose for dose-response assessment, which in turn will facilitate the identification of "bad actors" in the mixture. Identification of potential toxic components and their mode of action in turn will feed into decisions as to which components of the mixture should be the focus of more detailed kinetic investigations. Such an iterative process linking the pharmacokinetic with the pharmacodynamic aspects of the problem will narrow the scope of the modeling effort to allow quantification and prediction of the behavior of critical components of the mixture in the context of the rest of the fuel.
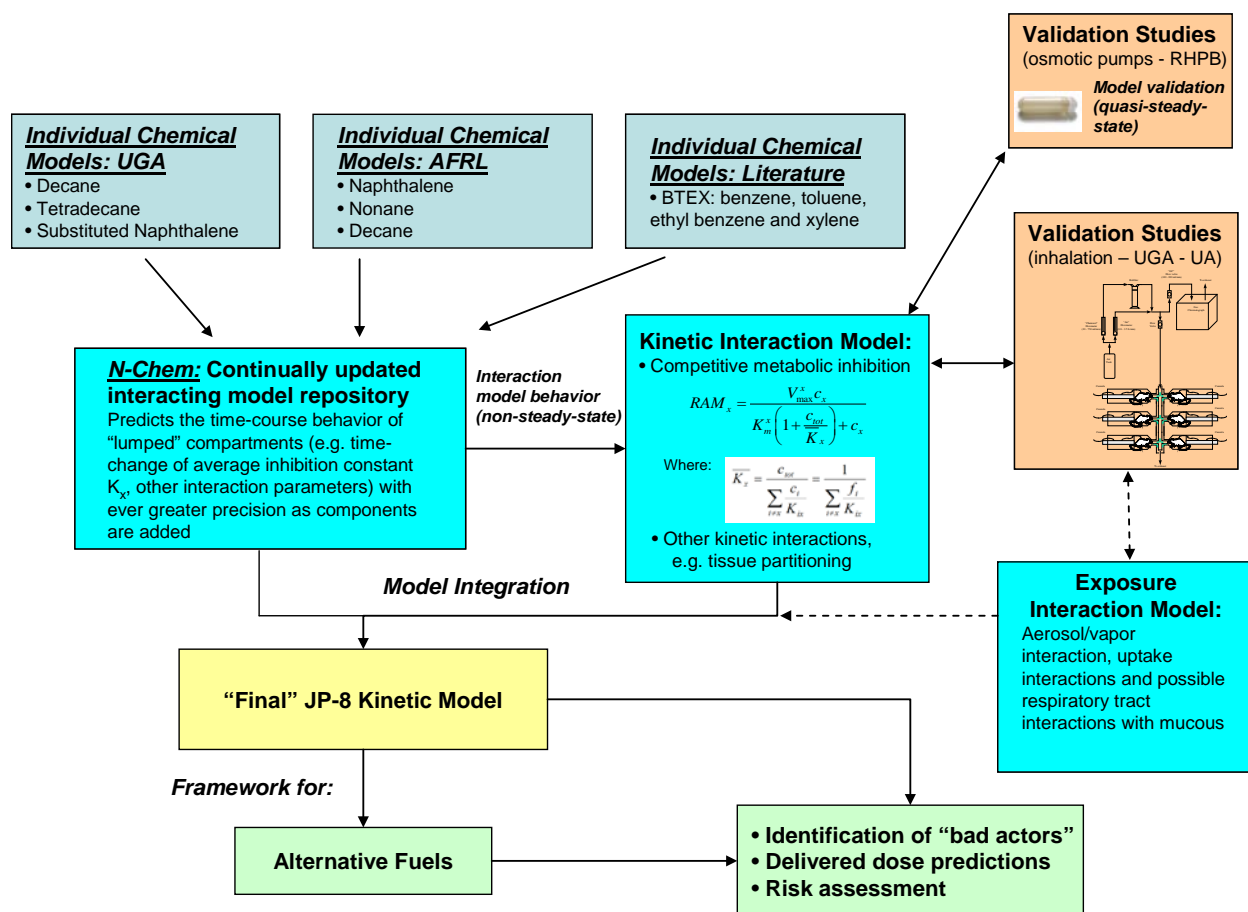
Figure 1. Framework for development of PBPK (physiologically based pharmacokinetic) model for complex mixtures (JP-8)

1

For FY08 (and overall) there were 4 Focus Areas:
1. Nonane/decane model finalization
2. Naphthalene model
3. Complex mixture model development and experimental program/model validation
4. Harmonized model framework/representative compound selection/modeling (collaboration with University of Georgia (UGA)) (including prediction of tissue PCs)

In FY 07 there were 3 main Focus Areas:
- Decane model
- Nonane model
- Naphthalene model

In FY 06, the first year of the project, there were 4 Focus Areas:
- Nonane/Decane Models
- Naphthalene Literature
- Harmonized Model Framework
- Complex mixture experimental program/model validation

The 4 overall Focus Areas are summarized below and discussed in more detail in separate sections to follow.

1. Nonane/decane models
Nonane and decane models have been developed and integrated into a single model structure. Features of the models include use of measured partition coefficients, multiple fat compartments, inclusion of dermal absorption in the model and scrubbing in the upper respiratory tract for inhalation exposure, and use of extended validation datasets. These models have been described in detail in a technical report (Robinson and Merrill, 2008) and two peer-reviewed publications (Merrill *et al.*, 2008; Robinson and Merrill, manuscript in preparation).

2. Naphthalene model
We translated a naphthalene physiologically based pharmacokinetic (PBPK) rat model from Advanced Continuous Simulation Language (ACSL) 11.8^{TM} (Aegis Technologies Group, Inc, Huntsville, AL) to acslXtreme^{TM} (Aegis Technologies Group, Inc, Huntsville, AL) and transitioned it to industry so they could use it to help address issues raised by the U.S. Environmental Protection Agency (U.S. EPA) review of the toxicity data for naphthalene. A simpler harmonized naphthalene model is in development; it has been added to the *n-chem* model (our continually updated repository of interacting PBPK models of JP-8 components in ACSL format). An animal use protocol was written in order to be able to determine experimental partition coefficients for naphthalene. Experiments to determine partition coefficients for this chemical have been conducted, but experimental difficulties have prevented the actual attainment of this objective.

3. Complex mixture model development and experimental program/model validation
We have developed a model of complex mixtures such as jet fuel in which interactions are modeled for the specific case of competitive metabolic inhibition of a specific enzyme (P450-2E1). In this model, the metabolic activity of a single chemical can be described as if it were one component of a simple two component mixture, with the other components appropriately "lumped." The total mixture concentration is sufficient to completely describe the interaction of each chemical with the rest of the mixture, via a specific, model-dependent average value for

the inhibition constant. This average value, in turn, can be successively approximated by measuring its value for specific representative components. This model is in the process of being validated in a series of experiments in which chemical components of JP-8, specifically nonane and naphthalene, are given to rats individually or in combination with JP-8 using an implanted osmotic pump that delivers a constant rate of chemical over a period of time, and the effect of the presence of JP-8 on the kinetics of the component is measured.

4. Harmonized model framework/representative compound selection/modeling
Harmonization is considered to be the imposition of a common model structure for a number of similar but distinct chemical components. In our case, we combine single chemical models into a single structure via appropriate interactions (initially limited to competitive metabolic inhibition in the liver). For a relatively small number of components, this constitutes a composite simple mixture ("n-chem") model. Further, we have developed a generic tissue compartment in which we have combined diffusion limitation and deep tissue (global tissue model). Such a tissue compartment can be simplified, if necessary, to apply to the interaction of specific compounds with specific tissues. We have also applied a QSAR approach for estimating blood and tissue partition coefficients, and in integrating our kinetic model with exposure models. This work is being done in collaboration with Dr. Jeff Fisher of the University of Georgia.

BACKGROUND

JP-8 is a kerosene-based fuel consisting of a complex mixture of hundreds of components from a number of hydrocarbon classes, including straight chain alkanes, branched chain alkanes, cycloalkanes, diaromatics and naphthalenes (Potter and Simmons, 1998). Human exposures to JP-8 in the vapor, aerosol and liquid forms all have the potential to be harmful. Situations where fuel becomes aerosolized have the greatest potential to be a hazard via inhalation. Both aerosol and liquid forms of JP-8 have the potential to cause local and systemic effects with prolonged or repeated skin contact. JP-8 exposure has been shown to result from aircraft engine starts at low ambient temperatures as a result of incomplete combustion (Pleil *et al.*, 2000). It may be inhaled, irritate the eyes or result in skin irritation and absorption. Potential JP-8 dermal exposure scenarios are:
- Prolonged contact with the skin of ground personnel through soaked clothing
- Splashes during refueling or fuel handling
- Handling engine parts which are coated with fuel
- Contact with sides of fuel tank during fuel tank maintenance operations
- Contact with fuel leaks on the underside of the aircraft or on the ramp

JP-8 components may interact in a number of ways, such as competing for the same metabolic enzymes, or modifying each others' partitioning into various tissues of the body. In order to fully characterize the behavior of any one component, one must simultaneously characterize the effects of all others. One way to explore these component interactions is to develop physiologically-based pharmacokinetic (PBPK) models of individual chemical components (Robinson, 2000) and then model these interactions (Focus Areas 1 and 2). However, with the large number of components, this becomes an impossibly complex undertaking. For example, a single type of (simple) binary interaction between 300 components would require the specification of some 10^5 interaction coefficients.

One proposed solution to this problem is to "lump" the components into a fewer number of groups consisting of "similar" chemicals according to some well defined chemical properties or

behaviors (such as equivalent carbon number, aliphatic or aromatic classification, molecular weight, water solubility, lipid partitioning, vapor pressure, etc.). Each group can then be characterized by examining in detail a chosen representative compound of that group; interactions between groups can be investigated by studying interactions between these representative compounds. This approach has been advocated, for example, by the Total Petroleum Hydrocarbon (TPH) Criteria Working Group, which has classified petroleum hydrocarbon fractions into six aliphatic and seven aromatic classes (Gustafson *et al.*, 1997). This approach is the basis for the work in Focus Area 4 in the present project.

Although it is useful as perhaps a first approximation, there are a number of difficulties with this "lumping" approach, including the problem that categorization criteria may be applicable to one type of behavior (such as blood-air partitioning), but may not be suitable for another (such as blood-tissue distribution). In addition, the composition of a group may change with time so that the properties of the group of chemicals as a whole may no longer be reflected by those of the originally chosen representative compound (Potter and Simmons, 1998). We therefore propose an alternative approach that retains some of the advantages of the "lumping" process, while allowing the changing properties of the mixture to be mathematically characterized. This approach consists of the development and validation of a complex mixture model, and forms the basis of the work described in Focus Area 3.

1. NONANE/DECANE MODEL

Introduction

As a first step in the development of a PBPK model for JP-8, we developed and modified models for some representative components of the mixture. In our laboratory we are focusing on PBPK models for nonane, decane and naphthalene, while octane, the longer chain aliphatic tetradecane, and substituted naphthalenes are being studied in the laboratory of Jeff Fisher at the University of Georgia. PBPK models for both nonane and decane were developed and integrated into a single model structure. Model components included:

- Use of measured partition coefficients
- Multiple fat compartments
- Incorporation of dermal absorption processes into the model
- Use of additional experimental datasets (including white spirit studies, since both decane and nonane are components of this mixture) in model development and validation

Data Analysis: Decane

Measured Partition Coefficients

A PBPK model for decane has previously been developed for n-decane (Perleberg *et al.*, 2004). Blood-air and tissue-blood partition coefficients have been measured by Zahlsen *et al.* (1992), Lof *et al.* (1999) and Smith *et al.* (2005), for a number of tissues including fat (see Table 1). In the Perleberg model, however, partition coefficients (PC) fitted to kinetic data from a four hour exposure were used in preference to these measured values. In particular, Perleberg *et al.* found it necessary to change the measured partition coefficient for fat from around 200-300 to 25, in order to fit their kinetic data. Such a large change in a critical parameter, without any

physiological basis, greatly impedes the model's extrapolative abilities, as well as its applicability for assessing the interactions of n-decane or similar alkanes with other compounds in a mixture model. Our approach therefore emphasized the use of experimentally determined PCs, in part also because many tissues had not approached steady-state concentrations by the end of the four hour exposures.

Table 1. Comparison of partition coefficients measured in Smith *et al. (*2005), Zahlsen *et al. (*1992) and Lof *et al. (*1999), and fitted values estimated in Perleberg *et al. (*2004).

	Measured Values		Fitted Partitions
	Vial Equilibration (*in vitro*) (Smith *et al.*, 2005)	*In Vivo* (Zahlsen *et al.*, 1992; Lof *et al.*, 1999)	Perleberg *et al.* (2004)
Blood/air	8.13	-	5.28
Liver	1.96	6.8 / -	6.52
Fat	328	181 / 250	25.54
Brain	4.8	8.8 / 3.4	3.41
Skin	5.00	-	1.20
Slowly perfused (muscle)	0.85	-	0.10
Richly Perfused (kidney)	-	11.4 / -	6.52

"-" indicates that the PC was not determined in the study.

Model Structure

Diffusion-limitation was used to describe decane kinetics in the brain, perirenal fat, skin and liver. Flow limitation was used to describe the remaining slowly perfused tissues. An overall schematic for our model is shown in Figure 2. This structure is similar to that of the previous model by Perleberg *et al. (*2004). In keeping with the goal of a harmonized modeling approach for representative compounds that can be combined for assessing mixtures, the model was both simplified and expanded. For simplification, compartments for bone marrow and spleen were lumped with the richly perfused tissues, as they did not improve predictions within target tissues such as brain, and as decane's role as an immunotoxicant has not been established (Vijayalaxami, personal communication). Similarly, earlier findings that JP-8 induced increased micronuclei in bone marrow have not been reproducible (Vijayalaxmi *et al.*, 2006). The model was expanded in aspects that would be critical for future evaluation of decane kinetics in a mixture context. This included the addition of dermal absorption and nonlinear metabolism in the liver. The perirenal fat, brain, skin and liver data for both alkanes demonstrate slow diffusion from the capillary beds into the tissue cells and/or slow diffusion out of the tissue. Therefore these tissues were described using two subcompartments to represent the tissue's cells and capillary bed. The rate of change in the associated tissue blood subcompartment equals the sum of the net retention from blood flow plus the net flux from cellular matrix, as shown below:

$$V_{Tb} \frac{dCV_T}{dt} = Q_T (CA - CV_T) + PA_T \left(\frac{C_T}{P_T} - CV_T \right)$$

$$V_T \frac{dC_T}{dt} = PA_T \left(CV_T - \frac{C_T}{P_T} \right)$$

where: V_{Tb} and V_T = volumes of tissue blood and tissue, respectively. Q_T = tissue blood flow, CA = arterial blood concentration, CV_T = concentration in the tissue's venous blood supply, PA_T = permeability area cross-product for absorption into tissue, C_T = concentration in tissue, and P_T = tissue to blood permeability coefficient.
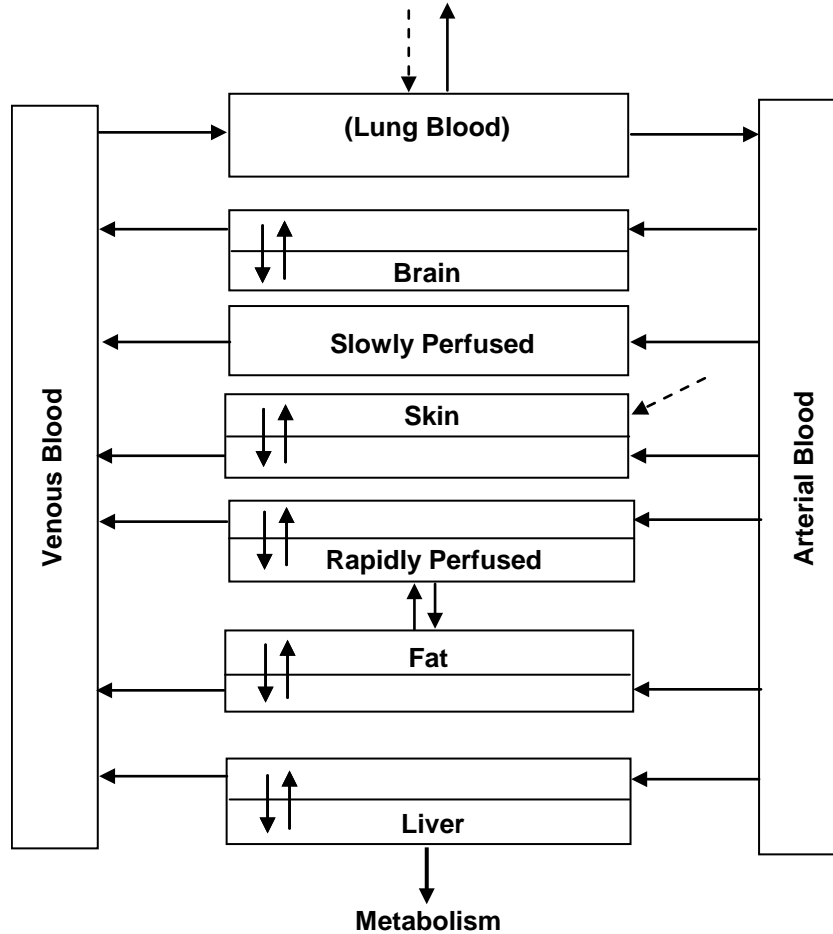
Figure 2. PBPK model of n-decane kinetics in the body. Fat, brain, skin, liver and rapidly perfused tissues are described by diffusion limitation; the slowly perfused tissues are described as flow limited. Exposure routes include inhalation and dermal absorption, as indicated by dashed arrows.

The slowly and richly perfused tissues were described as flow-limited compartments. The rate of change in the tissue concentration is perfusion-limited as described below:

$$V_T \, dC_T/dt = Q_T(CA - C_T/P_T)$$

As mentioned earlier, dermal absorption was included as the goal is to develop a representative model inclusive of common JP-8 exposure scenarios. Skin was described with diffusion-limitation across the capillary vesicles into tissue, as well as across the surface, as shown below:

$$V_{Sk} \, dCV_{Sk}/dt = (CA - CV_{Sk}) + PA_{Sk}\left(C_{Sk}/P_{Sk} - CV_{Sk}\right)$$

$$V_{SkB} \, dC_{Sk}/d_t = m \times Kp_{Sk} \times A_{Sk}\left(CIX - C_{Sk}/P_{Skf}\right) + PA_{Sk}\left(CV_{Sk} - C_{Sk}/P_{Sk}\right)$$

where: CV_{Sk} = concentration in dermal blood, PA_{Sk} = the permeability area cross product for skin, P_{Sk} = the skin:blood partition coefficient, V_{Sk} and V_{SkB} = the volumes of skin tissue and skin blood, respectively, Kp = the dermal permeability coefficient, m = modifying factor (see below), A_{sk} = the area of skin exposed and P_{Skf} = the surface:skin concentration ratio.

The rate of change in the amount in the liver was described by both flow limited diffusion, including metabolic loss via the cytochrome P-450 system, described by non-linear Michaelis-Menten kinetics as shown in the following equation:

$$dAmet/dt = \frac{Vmax \times C_L}{Km \times \left(1 + CV_L/Km + CV_{LX}/Km_X\right) + CV_L}$$

Intertissue diffusion between fat and liver is described below. It should be noted that the equation below includes competition for metabolism by other components, indicated by subscript x in the equation above.

$$V_L \, dC_L/dt = PA_L\left(CV_L - C_L/P_L\right) + KIL_F(C_F - C_L) - dAmet/dt$$

Where: $dAmet$ = change in amount metabolized, Km = M-M constant (mg/L), $Vmax$ = maximum capacity of decane, CV_{Lx} and Km_x = the concentration and M-M constants for other competing components of JP-8 in liver blood, respectively. C_L = concentration in liver, PA_L = permeability area cross product for liver and KIL_F = intertissue diffusion rate between fat and liver.

The model's differential equations were coded in Advanced Continuous Simulating Language (ACSL™, Aegis Technologies Group, Huntsville, AL) and solved simultaneously.

Model Parameterization

The blood flows, tissue volumes and tissue blood volumes used in the model (Table 2) were obtained from Brown *et al. (*1997). Alveolar ventilation was estimated to be higher than cardiac output, assuming the animals are in various positions and slightly stressed. Even with healthy

animals, changes in postures can result in slight mismatches between ventilation and perfusion, due to some alveoli being relatively over-ventilated while others are relatively over-perfused. Partition coefficients were obtained from the literature, while permeability - tissue capillary surface area cross products (*PA*) for diffusion limitation (Table 3) were visually optimized by fitting predicted tissue concentration-time curves to experimental data.

Table 2. Physiological parameter values for the decane model

Parameter	Name	Rat	Human
BW	Body weight (kg)	0.3	70.0
Q_C	Cardiac output (blood flow) (L/(hr kg))	15	16.5
Q_P	Alveolar ventilation (L/(hr kg))	24.8	29.0
Blood Flows to Tissues [fraction of Q_C]			
Q_L	Liver	0.25	0.23
Q_F	Fat	0.09	0.052
Q_{Br}	Brain	0.03	0.114
Q_{Sk}	Skin	0.02	0.058
Q_R	Rapidly perfused $0.76\text{-}Q_L\text{-}Q_{Br}$	0.48	0.42
Q_S	Slowly perfused $0.24\text{-}Q_F\text{-}Q_{Sk}$	0.13	0.13
Tissue volumes [fractions of BW]			
V_L	Liver	0.04	0.026
V_F	Fat	0.09	0.21
V_{Br}	Brain	0.0057	0.02
V_{Sk}	Skin	0.19	0.037
V_B	Alveolar blood	0.007	0.008
V_R	Rapidly perfused	0.064	0.078
V_S	Slowly perfused	0.47	0.40
Tissue blood volumes [fractions of tissue volumes]			
V_{LB}	Blood fraction of liver	0.21	0.11
V_{FB}	Blood fraction of fat	0.02	0.02
V_{SkB}	Blood fraction of skin	0.08	0.08
V_{BrB}	Blood fraction of brain	0.03	0.04
V_{RB}	Blood fraction of rapidly perfused tissue	0.21[a]	0.21[a]

Values from Brown *et al.* (1997). This table was taken from Merrill *et al.* (2008).
[a]Based on blood fraction of kidneys

Table 3. Chemical-specific parameter values for the decane model

Partition Coefficients	Value
P_B Blood:air	5.0[a]
P_L Liver:blood	1.97[a]
P_F Fat:blood	328[a]
P_{Br} Brain:blood	4.8[a]
P_{Sk} Skin:blood	5.0[b]
P_{Skf} Surface:Skin	150[c]
P_S Slowly perfused (muscle):blood	0.85[a]
P_R Rapidly perfused (kidney):blood	3.00[d]
Diffusion rates	
PA_F permeability area cross product - fat absorption (L/hour)	0.7[c]
PA_L permeability area cross product - liver (L/hour)	0.15[c]
PA_{SK} permeability area cross product – skin (L/hour)	0.02[c]
PA_{Br} permeability area cross product – brain (L/hour)	0.009[c]
PA_R permeability area cross product – rapidly perfused (L/hour)	1.0[c]
$Vmax$ maximum velocity of saturable metabolism (mg/hour-kg)	0.4[c]
Km Affinity of saturable metabolism (mg/L)	1.5[e]
Kp_{Sk} Dermal permeability coefficient (cm/hour)	1.11[f]
m Modifying factor for Kp_{Sk} (unitless)	0.001[c]
K_{RF} Rapidly perfused-fat intertissue transfer rate (L/hour)	0.0002[c]
K_{FR} Fat-Rapidly perfused intertissue transfer rate (L/hour)	0.00005[c]

This table was taken from Merrill *et al.* (2008).
[a] Smith *et al.* (2005)
[b] Perleberg *et al.* (2004)
[c] visually optimized to available kinetic as described in methods
[d] Zahlsen *et al.* (1990)
[e] Mortensen *et al.* (2004)
[f] NIOSH Skin Permeation Calculator, Modified Robinson Model (accessed Sept. 2007)
Notes: The tissue:blood partition coefficient (PC) values used for slowly and rapidly perfused were derived from muscle:blood and kidney:blood PCs, respectively (Smith *et al.*, 2005; Zahlsen *et al.*, 1990; Lof *et al.*, 1999). Bone mass was not included in volume estimates of richly or slowly perfused tissue.

With partition coefficients set to measured values provided in Table 3, visual fitting of the remaining diffusion rates, referred to as permeability area cross products (*PA*s), was an iterative process beginning with fat. Due to its lipophilicity, decane is stored in fat and slowly released, affecting its kinetics in other tissues greatly. Therefore the permeability cross product for fat (*PA_F*) was visually optimized to the Perleberg *et al.* fat data from the 1200 ppm dose group. Similarly, the PA values for skin, liver and brain were visually fit to their respective data from the same study while all other parameters held constant. It was then found that inclusion of a low intertissue diffusion rate between fat and liver (*KI_FL*) improved model fits.

In the case of skin, dermal permeability coefficients (*Kp*) representing absorption from a vapor medium are not available. Therefore the *Kp* used represents permeability from direct contact with a liquid media, which would certainly overestimate the potential absorption from vapor exposures, possibly by orders of magnitude. Therefore, a modifying factor (m) was used to reduce the permeability coefficient to an extent representative of dermal permeability from a vapor media. To parameterize *m* and PA_{Sk}, *m* was initially set to zero while all other parameters held constant to those listed in Table 2 and the permeability area cross product (PA_{Sk}) was visually fitted to the skin kinetic data at 1200 ppm. Then m was adjusted to improve the model fit. The *m* value had to be maintained at a very low value of 0.001 or less, indicating that the sequestration of n-decane in skin from vapor exposures occurred mainly via systemic circulation. However, as mentioned, due to direct dermal contact to liquid hydrocarbons, dermal permeation is expected to contribute considerably to decane sequestration via dermal permeation. Unfortunately, data were not available to validate the Kp value taken from the NIOSH skin permeability calculator.

Michaelis-Menten liver metabolic constants for n-decane have been measured (*Km* = 1.5 mg/L and *Vmax* = 0.4 mg/hour) using rat liver slices in a vial head-space equilibration system (Mortensen *et al.*, 2000). Their data indicate that clearance via liver metabolism is minimal for n-alkanes, which, in addition to their lipophilicity, contributes to their tendency toward increased body retention. During our model development, we found that decane cleared the liver biphasically, similar to blood, and the addition of metabolic clearance only resulted in underestimation of liver concentrations. Therefore, the *Vmax* value was set to zero. Instead of removing the metabolic pathway from model code, it was retained as part of a harmonized model structure as it would be critical in predicting kinetics of other non-saturated JP-8 components, such as aromates.

Results

Results of fitting the model to the available decane data, using experimental partition coefficient values from Table 3, are shown in Figures 3 and 4 for the data of Perleberg *et al. (*2004) and Zahlsen *et al. (*1992), respectively. Note that all parameters are the same across the two datasets, including the value for fat diffusion, PA_F = 0.7 L/hour (see Table 3). While such a value works for the Zahlsen data, a lower value of 0.06 L/hour results in the fit to the fat data of Perleberg *et al. (*2004) shown in Figure 3. The data seem to suggest that that fat uptake is slower at higher concentrations (see discussion below).
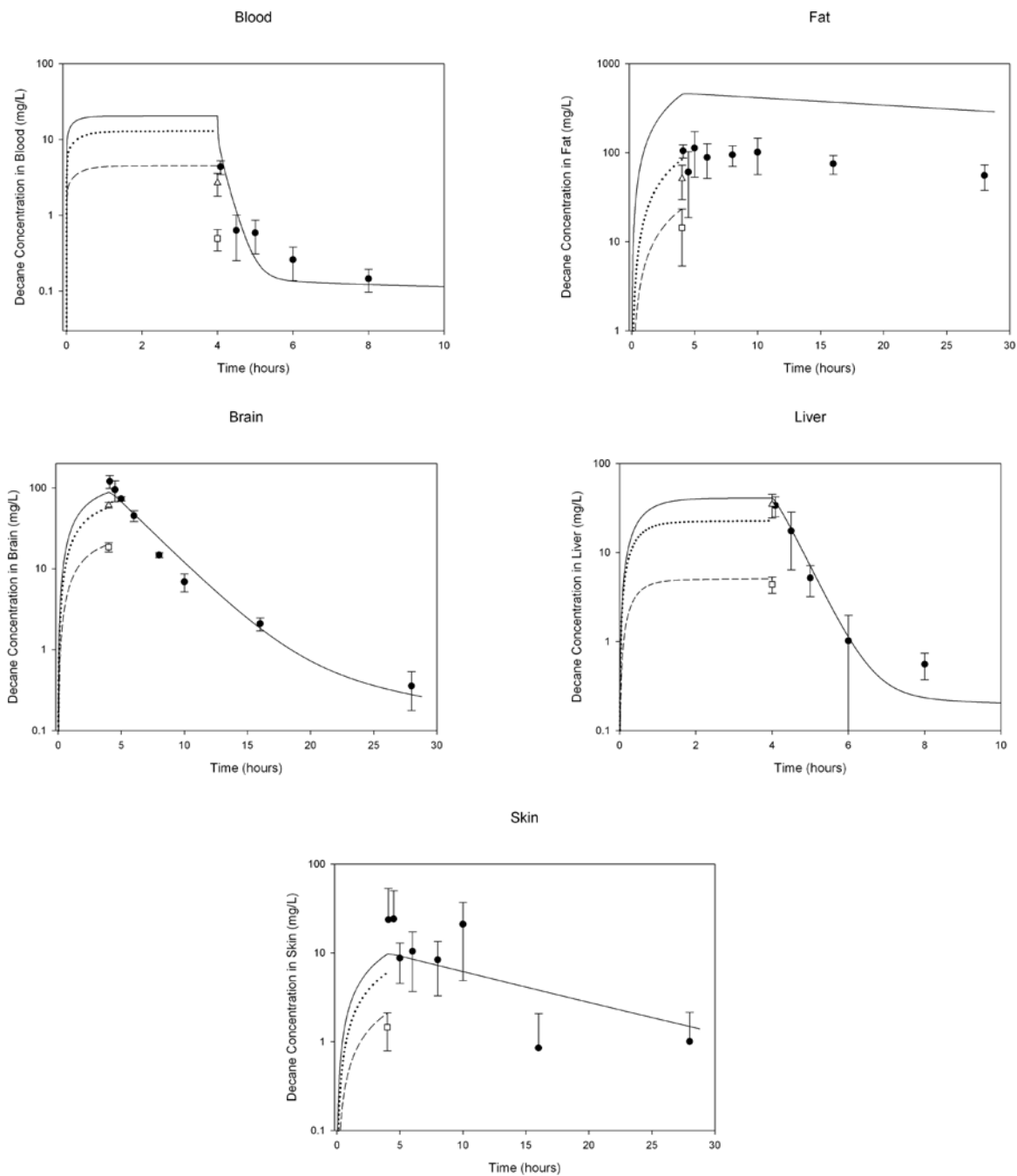
Figure 3. Model predictions (lines) of decane concentrations in tissues (mg/L) over time (hours) versus Perleberg *et al. (*2004) data. Points and bars indicate mean and standard deviations. Rats were exposed in closed chamber to 1200 (solid line, filled circle), 781 (dotted line, open triangle) & 273 ppm (dashed line, open square) for 4 hours. End-of-exposure time points only were collected for the 781 and 273 ppm dose groups; skin data for the 781 ppm dose group were not available.
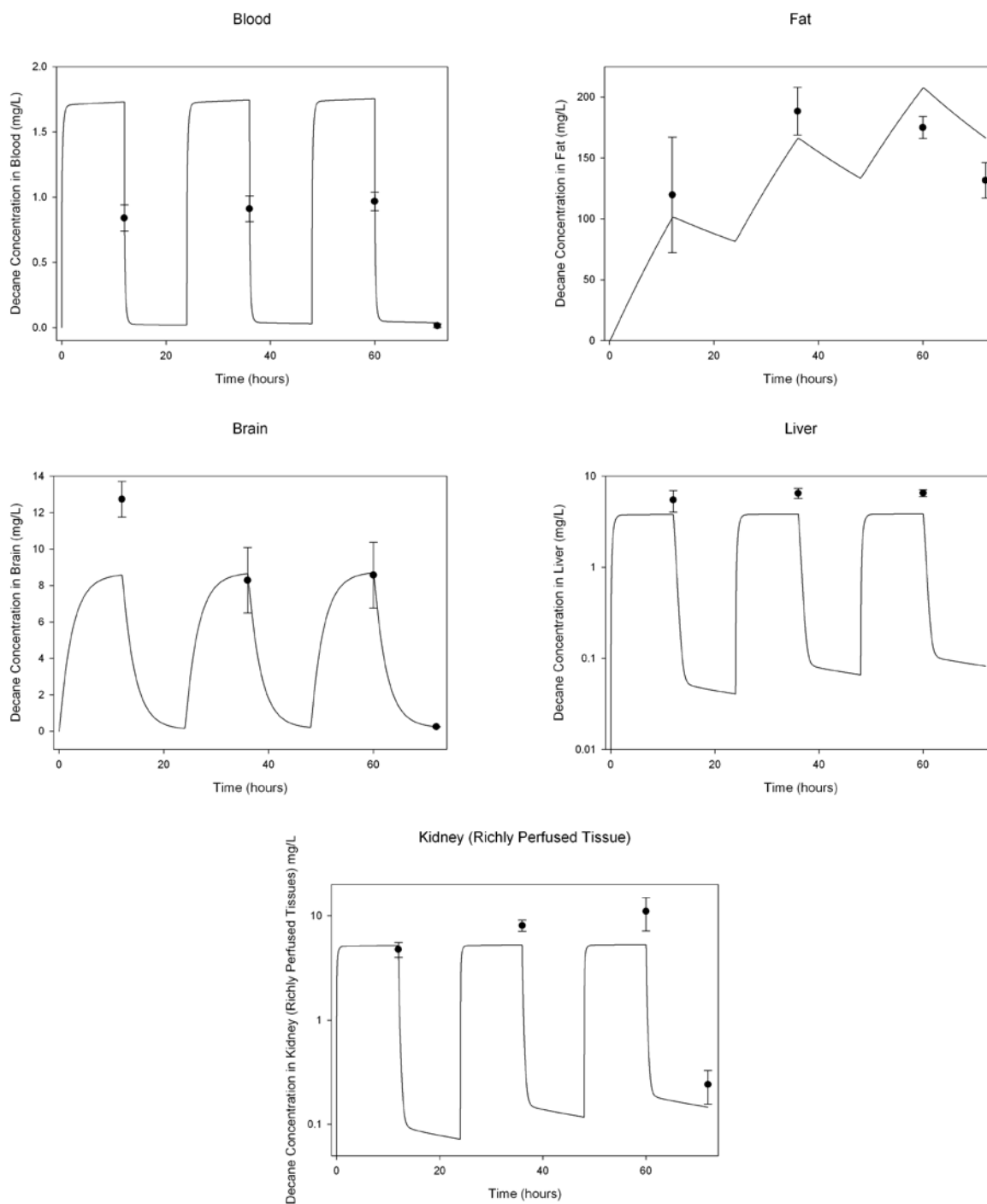
Figure 4. Model predictions (lines) of decane concentrations (mg/L) over time (hours) versus measured data from Zahlsen *et al.* (1992). Rats were exposed to 100 ppm, 12 hours/day. PA_F = 0.7 L/hour.

Figure 5 shows the fit of our decane model (with no adjusted parameters) to the white spirit data of Lof *et al. (*1999). Exposures were 400 and 800 ppm white spirits for 6 hours/day for 3 weeks (n=5), which is equivalent to 106 and 212 ppm decane. The model underpredicts the measured data for blood and fat, and overpredicts brain, but is well within an order of magnitude of each and mimics the trend of the data well. The simulations and data suggest that perhaps the decane concentration in the vapor mixture is in fact higher than in the liquid white spirits. This is a reasonable hypothesis given decane's higher volatility in comparison with larger branched and cyclic aliphatics in the mixture. The data may also suggest competition for partitioning in the tissues. In fact, competition for uptake into tissues has been shown with similar compounds. Zahlsen and others (1993) examined tissue uptake from equal concentrations of n-nonane, naphthenes and aromatics, and found greater uptake of aromatics and naphthalenic compounds in blood, brain and fat than alkanes.

It should be noted that Lof *et al. (*1999) reported sedation at 400 ppm of dearomatized white spirits during the first day, from which the animals recovered through the week. Perleberg and colleagues did not report on possible anesthetic effects at 1200 ppm for 4 hours. However, at such a high exposure level, anesthetic effects are expected, despite the difference in chemical composition between dearomatized white spirits and pure n-decane. Anesthesia is known to alter blood flows. Stanek *et al. (*1988) reported significant decrease in flow to kidneys and the GI tract, while flow increased significantly to the brain, heart and liver during ether anesthesia. Although not measured, one would also suspect a decrease in flow to fat, as the body attempts to maintain adequate circulation to vital organs. Such an effect would effectively result in decreased diffusion into fat (i.e., decreased PA_F) at high exposures. This might explain what appears to be slower diffusion of decane into fat at 1200 ppm than at 100 ppm.

In addition, Lof *et al.* reported an increase in total brain dopamine (DA) at 800 ppm, and a decrease in serotonin (5-HT) at both 400 and 800 ppm during the first week of exposure. The catecholamine levels returned to normal the following week. Norepinephrine levels did not change significantly. Dopamine is known to cause vasodilation and decreased systemic blood pressure at low doses (Brodde, 1982). We believe dopamine's effect in this study is very transient because it is also a precursor to norepinephrine, which did not increase. The changes in serotonin levels may be of some significance in the modeling of blood flow in these studies as well as assessing liver toxicity from petroleum mixtures, since it was decreased at both exposure concentrations. Serotonin not only plays a role in CNS effects, such as mood, appetite and sexuality, but it has recently been identified as a potent mitogen (Lesurtel *et al.*, 2006), enhancing liver regeneration. Therefore, hypothetically, a decrease in serotonin could support a decreased blood flow to the liver and possibly decreased metabolism of competing compounds.
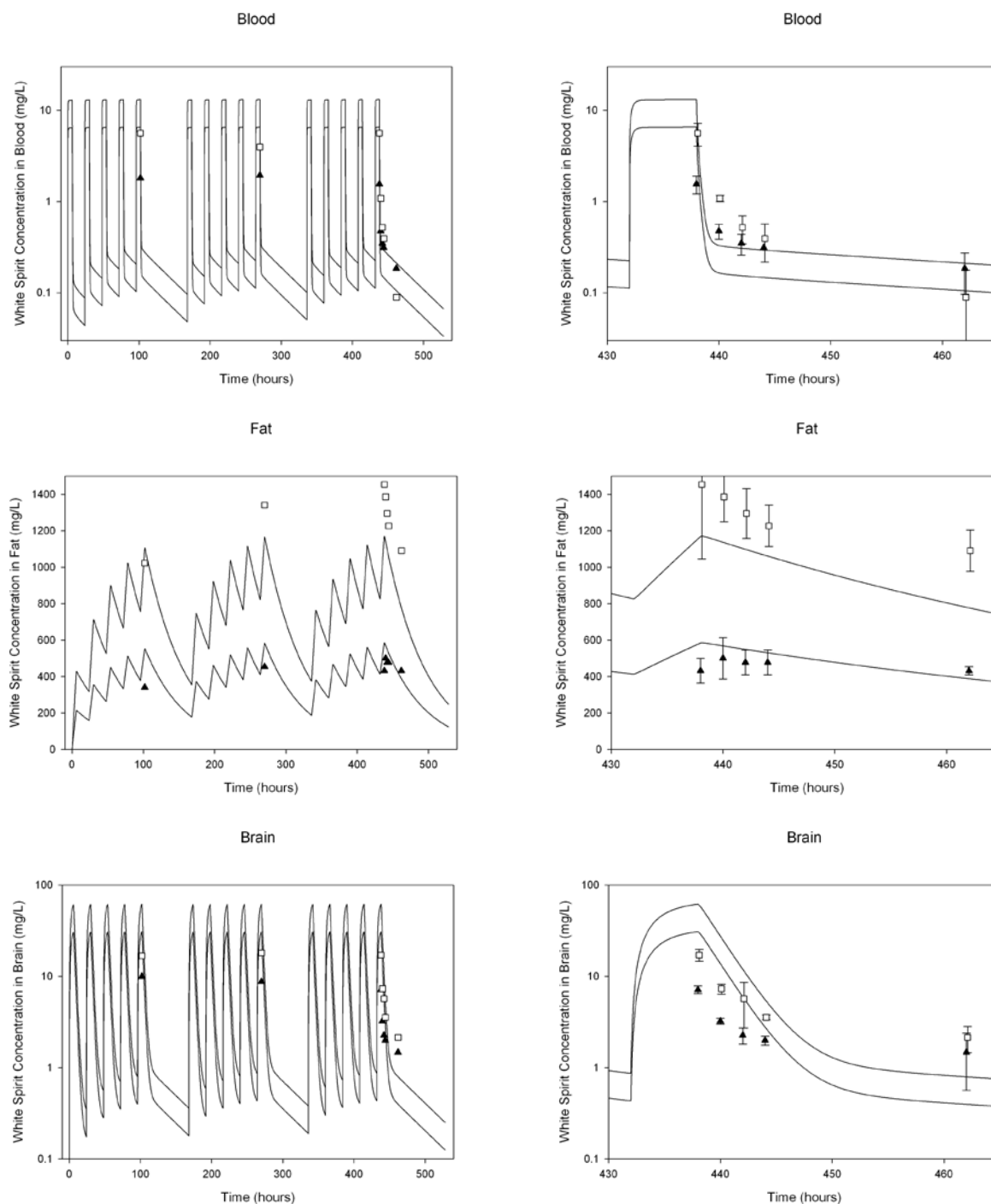
Figure 5. Model predictions (lines) of decane concentrations (mg/L) from white spirit over time (hours) versus measured data from Lof *et al.* (1999). Model predictions (lines) vs. measured total white spirits concentrations (mean values) in blood, fat and brain (Lof *et al.*, 1999). Rats were exposed 6 hours/day, 5 days/week for 3 weeks to 400 (triangles) and 800 ppm (squares) dearomatized white spirit. For each tissue, the simulation of the final peak on the last day of exposure and its clearance are shown on the right, with measured data and bars (mean and standard deviation).

Multiple Fat Compartments

Despite the added complexity, it became apparent that multiple fat compartments are needed for single-chemical models in order to adequately describe the data. In PBPK models, fat is generally described as a single (or sometimes two) homogeneous, poorly perfused compartment, which is assumed, like other tissues, to be in equilibrium with venous blood at a concentration determined by the fat-blood partition coefficient. For highly lipophilic compounds, such as those under consideration here, this description may not be accurate. Unlike other tissues such as liver or brain, fat is distributed throughout the body. Some fat is indeed concentrated in specific locations (such as perirenal fat), but other fat deposits are located within other tissues. It is feasible to consider that lipophilic compounds that distribute preferentially into fat may do so directly from the associated tissues without first going into the blood. Further, the fat in the body (even those deposits associated with specific tissues) may be considered at least partially "connected," in that material may move from one tissue region to another wholly within the fat, rather than first partitioning out into the blood (which such highly lipophilic compounds are indisposed to do).

Thus, based on these considerations, we devised an alternative model structure for such compounds that involves an expanded description of the fat, using an intertissue diffusion rate. Such a structure is shown in Figure 6. Transfers by intertissue diffusion mean that a small part of both richly and slowly perfused tissues are slower to reach equilibrium because the chemical (decane in this case) is continuously lost to adjacent fat. As a result there is also a decrease in the amount returning from these tissues to the blood and lungs. This phenomenon may explain the slight increase in liver decane and large increase in fat decane concentrations seen from day 1 to 3 in the study by Zahlsen *et al. (*1992). In their study, rats were exposed in closed chamber to 100 ppm decane, 12 hours/day for 3 days. During the exposures, blood and brain concentrations appear to have reached steady state conditions after the first day's exposure, while levels in fat continued to rise significantly and liver levels rose slightly through day 3. Using the approach in Figure 6 between liver and fat, we were able to capture this trend in the data (Figure 4). Without this intertissue diffusion, both would have reached steady state much sooner.
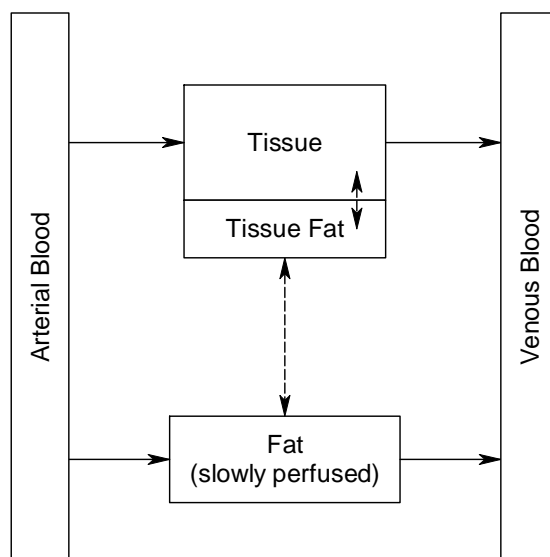
Figure 6. Schematic representation of multiple fat compartments, including those associated with specific tissues such as the liver

Both nonane and decane are highly lipophilic compounds (calculated log octanol-water partition coefficients = 4.76 and 5.25, respectively), which have been observed to distribute preferentially in brain, bone marrow and fat tissue (Perleberg *et al.*, 2004; Merrill *et al.*, 2008). Published PBPK models for nonane and decane have considerable limitations. For example, the nonane model by Robinson (2000) is oversimplified for direct application to various aliphatic hydrocarbons, lacking diffusion limitation in the fat and brain compartments, and while it successfully predicts nonane in blood and brain, it lacks validation against other tissues important in nonane's kinetics (i.e., fat and liver). The decane model developed by Perleberg and colleagues (2004) uses visually fitted tissue:blood partition coefficients vs. experimentally determined values and overpredicts experimentally determined fat concentrations by an order of magnitude, at occupational-relevant exposure concentrations.

In order to develop a common, harmonized structure (see "Harmonized Model Framework" below) for both the nonane and decane models, we therefore allow diffusion limitation for the fat, brain, skin and liver compartments. Further, we allow binding to components in the blood, such as erythrocytes and lipoproteins. We also permit scrubbing of the inhaled fuel by the mucous lining of the upper respiratory tract (URT). Finally, since dermal absorption of JP-8 is a significant route of exposure, both the nonane and decane PBPK models were extended to take this route of exposure into account.

Application of Decane Model to Humans

Extrapolation to humans was performed by changing physiological parameters to those listed in Table 2, which represent humans. No changes in chemical specific parameters were made, as no human kinetic decane data were available for parameterization. The fat diffusion rate, PA_F, was kept at 0.7. No human studies involving exposure to n-decane alone are available.

16

Therefore, for validation purposes, data of human exposures to white spirits by Pedersen *et al.* *(*1984) and Astrand *et al. (*1975) were used.

Pedersen *et al. (*1984) exposed 7 volunteers to 100 ppm white spirit (described as containing over nearly 99 percent aliphatic alkanes (C8–C12) for 6 hours/day for 5 days and collected venous blood and subcutaneous adipose biopsies from the underside of an abdominal skin fold, using needle aspiration. The biopsies were aspirated within approximately 15 minutes post cessation of daily exposures and then again 2 days after day 5 of exposure. Without knowledge of the mixture's n -decane content, we assumed that (as seen with the rat data) the majority of paraffin components in the exposure vapors would be highly volatile n -alkanes, and therefore would display biokinetics similar to n-decane. Hence, we simulated an exposure of 100 ppm and compared it with the measured fat and blood white spirit concentrations (see Figure 7). A PA_F value of 0.7 L/hour, scaled to $BW^{3/4}$, was used to remain consistent with the biochemical parameters used for simulating the low-dose (100 ppm) rat exposures. Figure 7 also shows the improvement of the fit to the fat data of increasing PAF to 3.0 L/hour.
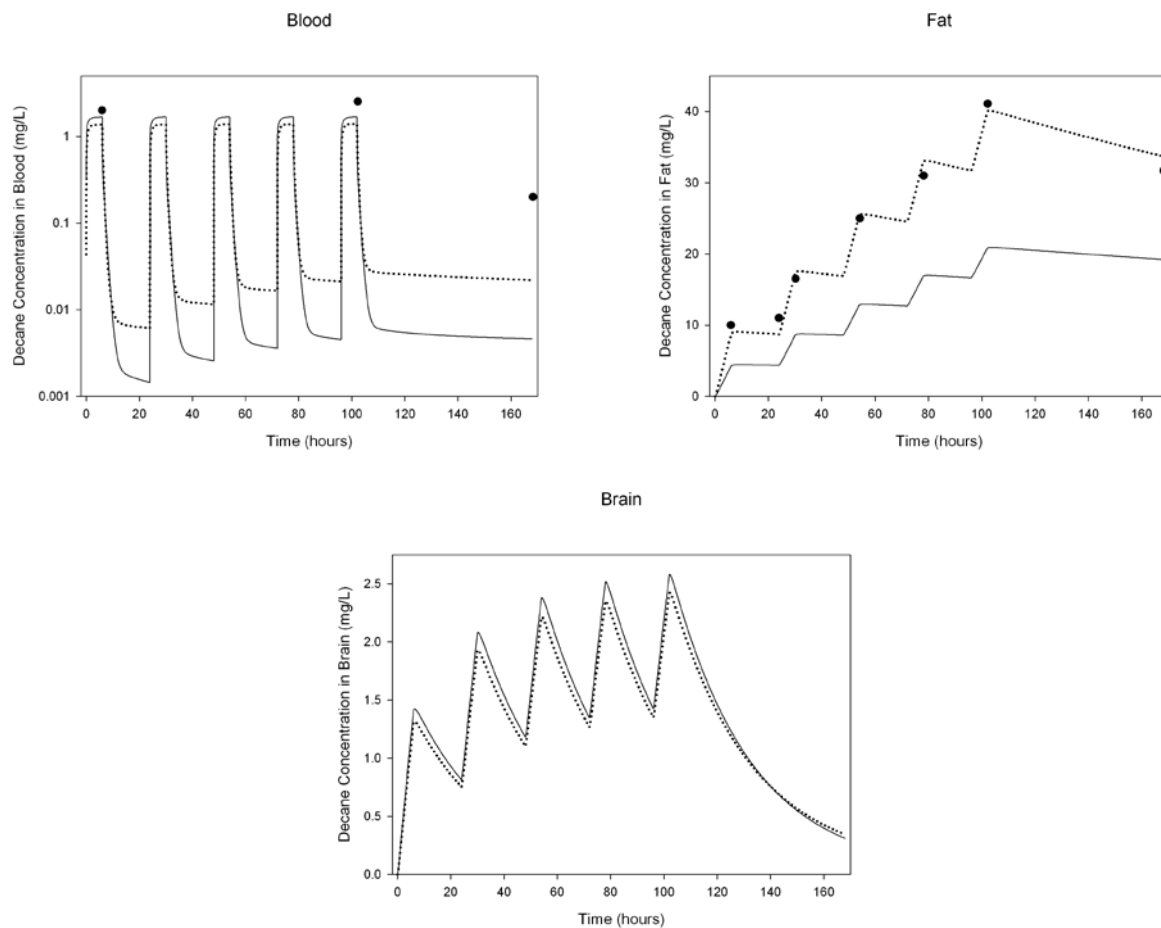
Figure 7. Model predictions (lines) of decane concentrations in tissues (mg/L) over time (hours) versus measurements of white spirits (circles) in blood and fat from daily 6-hour exposures to dearomatized white spirit for 5 days, together with model predictions for the brain. Solid lines are predictions for the parameters in Table 3 above, while dotted lines represent an increase in PA_F to 3.0 L/hour (see text). (Data from Pedersen *et al.*, 1984; figures from Merrill *et al.*, 2008)

The study by Astrand *et al.* (1975) involved exposing volunteers to 1250 ppm white spirits for 30 minutes. Based on the composition of the white spirits mixtures reported in the World Health Organization's Environmental Health Criteria 187 on White Spirit (Stoddard Solvent), we estimated a content of 30.3 ppm n-decane. At end of exposure, Astrand and colleagues measured an alveolar air concentration that was approximately 50 percent of the inspired air concentration (near 625 ppm). Using an exposure concentration that accounts only for the n-decane portion (30.3 ppm) for 30 minutes, our model predicted an expired air concentration of 16.9 ppm, which is 55 percent of 30.3 ppm. Again our model prediction is well within the proximity of measured value of a different parameter, expired air.

Data Analysis: Nonane

Nonane typically occurs in JP-8 at levels around 0.8 percent and has an octanol-water partition coefficient (Kow) of 5.65. It is metabolized to 2-nonanol by P450 enzymes, and further to 2-nonanone by alcohol dehydrogenase. An earlier analysis of the nonane data is described in a previous technical report (Robinson, 2000). This analysis was improved based on the harmonized decane-nonane model approach described below in the current report. In the following simulations, all fitted parameters were maintained with exception of partition coefficients and dermal Kp, which were changed to experimentally determined values for nonane.

Supporting Data and Results

Caracci 1995 unpublished data. In this 1995 unpublished in-house study, rats were exposed using a nose-only inhalation apparatus to 100, 500 or 1000 ppm for a period of 4 hours. The preliminary results of simulating these data with a nonane PBPK model with the same structure as that described for decane (Figure 2) are shown in Figure 8. Physiological and kinetic parameters are shown in Tables 4 and 5. The data from this study have been included for technical report publication in Robinson and Merrill (2008).
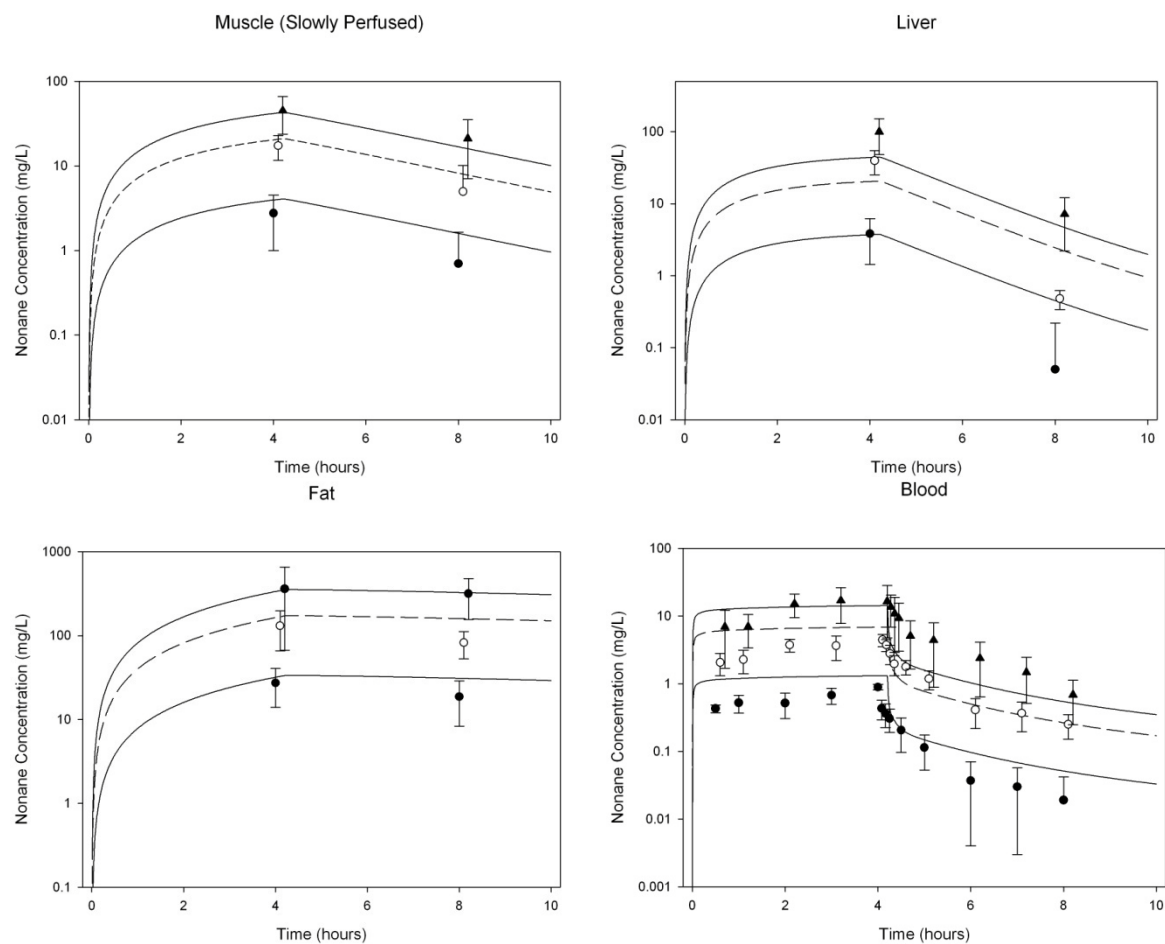
Figure 8. Model simulations (lines) of nonane concentrations in tissues (mg/L) over time (hours) versus measured nonane concentrations in muscle, liver, blood and fat from nose only exposures to 1000 (upper solid lines and circles), 500 (dashed lines and open circles), and 100 ppm nonane (lower solid lines and circles) for 4 hours (Caracci, 1995, unpublished data).

Table 4. Physiological parameter values for the nonane model

Parameter	Name	Rat
BW	Body weight (kg)	0.3
Q_C	Cardiac output (blood flow) (L/hour-kg)	15
Q_P	Alveolar ventilation (L/hour-kg)	24.8
Blood Flows to Tissues [fraction of Q_C]		
Q_L	Liver	0.25
Q_F	Fat	0.09
Q_{Br}	Brain	0.03
Q_{Sk}	Skin	0.02
Q_R	Rapidly perfused 0.76-QL-QBr	0.48
Q_S	Slowly perfused 0.24-QF-QSk	0.13
Tissue volumes [fractions of BW]		
V_L	Liver	0.04
V_F	Fat	0.09
V_{Br}	Brain	0.0057
V_{Sk}	Skin	0.19
V_B	Alveolar blood	0.007
V_R	Rapidly perfused	0.064
V_S	Slowly perfused	0.47
Tissue blood volumes [fractions of tissue volumes]		
V_{LB}	Blood fraction of liver	0.21
V_{FB}	Blood fraction of fat	0.02
V_{SkB}	Blood fraction of skin	0.08
V_{BrB}	Blood fraction of brain	0.03
V_{RB}	Blood fraction of rapidly perfused	0.21[1]
V_{SB}	Blood fraction of slowly perfused	0.04[1]

Source: Brown *et al. (*1997)
[1] based on blood volumes of kidney and muscle for rapidly and slowly perfused, respectively

Table 5. Chemical-specific parameter values for the nonane model

Partition Coefficients	Value
P_B Blood/air	5.2[R]
P_L Liver/blood	3.5[Z]
P_F Fat/blood	282[R]
P_{Br} Brain/blood	5.0[S]
P_S Slowly perfused (muscle)/blood	4.0[Z]
P_R Rapidly perfused (kidney)/blood	2.0[Z]
P_{Sk} Skin/blood	4.0[D]
Diffusion Rates	
PA_F permeability area cross product - fat absorption (L/hour) (Zahlsen *et al.*, 1990 data)	0.7[f]
PA_F permeability area cross product - fat absorption (L/hour)	0.8[f]
PA_L permeability area cross product - liver (L/hour)	0.07[f]
PA_{Sk} permeability area cross product – skin (L/hour)	0.4[Df]
PA_{Br} permeability area cross product – brain (L/hour)	0.5[f]
PA_R permeability area cross product – rapidly perfused (L/hour)	1.0[f]
PA_S permeability area cross product – slowly perfused (L/hour)	0.5[f]
Vmax maximum velocity of saturable metabolism (mg/hour)	0.0[f]
Km Affinity of saturable metabolism (mg/L)	1.5[M]
K_{RF} Rapidly perfused-Fat intertissue transfer rate (L/hour)	0.00001[f]
K_{FR} Fat-Rapidly perfused intertissue transfer rate (L/hour)	0.0005[f]

[R] Robinson (2004)
[M] Mortensen *et al. (*2000)
[D] Based on skin data of Perleberg *et al. (*2004)
[Df] Based on fitted decane concentration in skin Merrill *et al.*, 2008)
[f] visually optimized to available kinetic data
[S] Based on value for decane Smith *et al. (*2005)
[Z] Zahlsen *et al. (*1992)
The tissue:blood partition coefficient (PC) values used for slowly and rapidly perfused were derived from muscle:blood and kidney:blood PCs, respectively (Zahlsen *et al.*, 1990; Lof *et al.*, 1999; Smith *et al.*, 2005).

Zahlsen et al. (1992). Rats were exposed in a closed chamber to 100 ppm nonane, 12 hours daily for 3 days. Preliminary simulations of these data are shown in Figure 9.

Zahlsen et al. (1990). Figures 10 and 11 show rat brain and blood nonane concentrations following exposure at 1000 ppm, 12 hours daily, for up to 14 days.
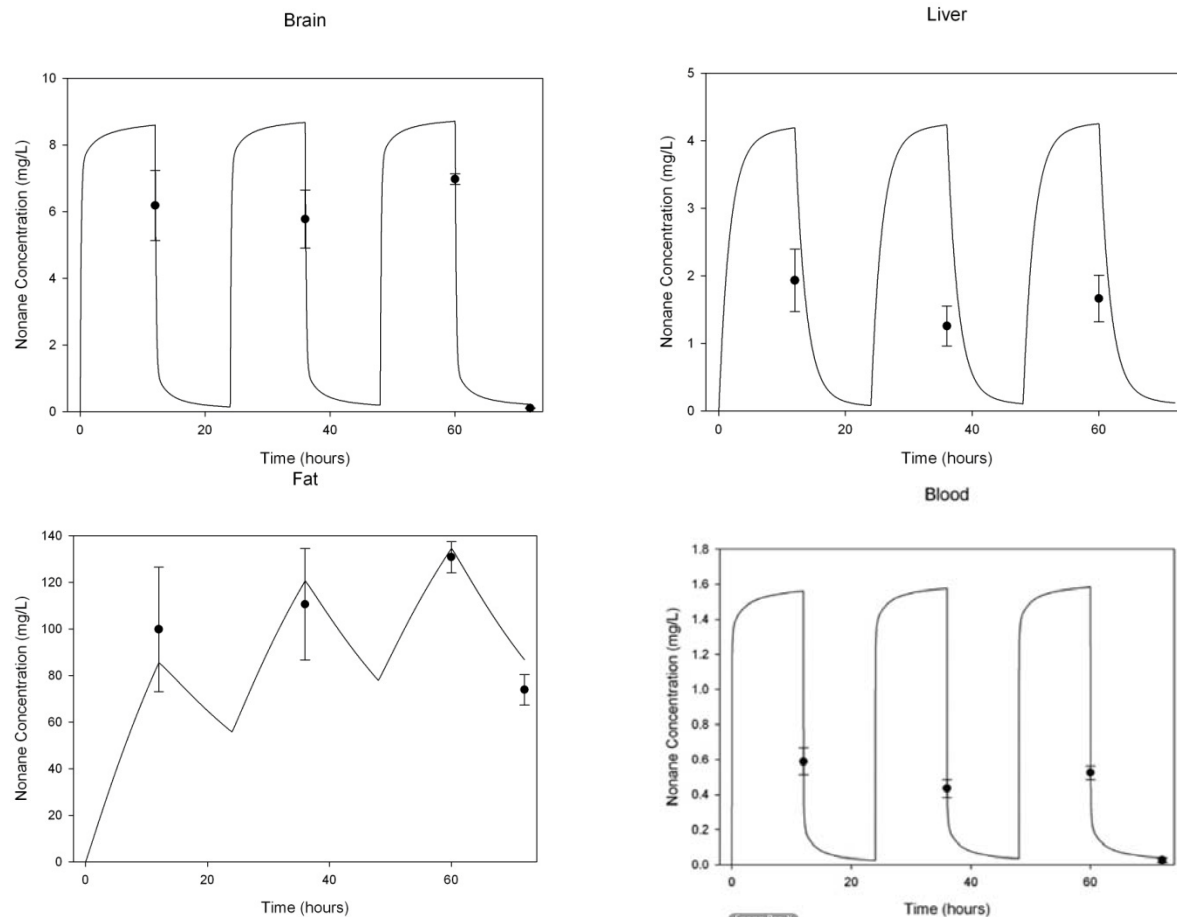
Figure 9. Model simulations (lines) of nonane concentrations (mg/L) over time (hours) versus measured nonane concentration (circles) in blood, fat, brain and liver in rats exposed in closed chamber to 100 ppm n-nonane, 12 hours/day, for 3 days. Data (mean ± SD) are from Zahlsen *et al. (*1992).
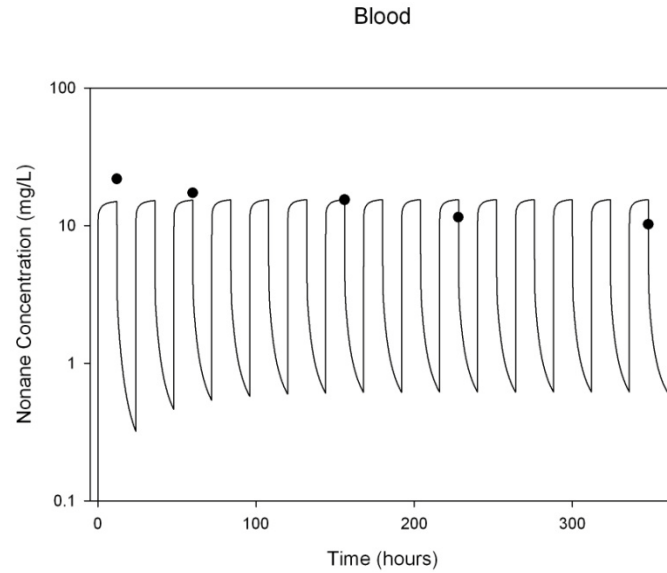
Blood

Figure 10. Model prediction (lines) of rat blood nonane concentration (mg/L) over time (hours) for the exposure scenario of Zahlsen *et al. (*1990) (1000 ppm, 12 hours daily for up to 14 days). Data are adapted from Figure 1 of that paper.
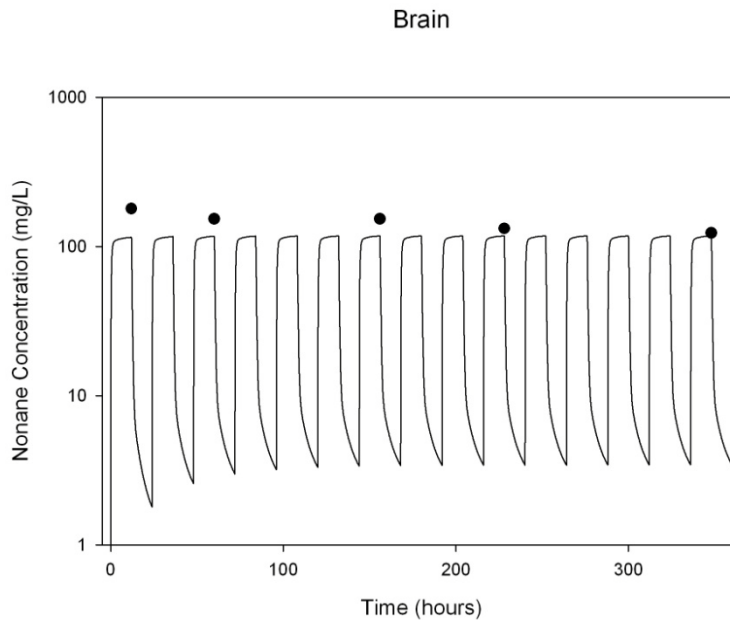
Brain

Figure 11. Model prediction (lines) of rat brain nonane concentration (mg/L) over time (hours) for the exposure scenario of Zahlsen *et al. (*1990) (1000 ppm, 12 hours daily for up to 14 days) using measured and previously fitted parameter values. Data are adapted from Figure 2 of that paper.

This model is presented in the technical report (Robinson and Merrill, 2008, *A Harmonized Physiologically-Based Pharmacokinetic Model for Nonane as a Component of Jet Fuel*). Single-chemical models such as those for nonane and decane can be "harmonized" (same physiological structure) and combined into a composite mixture model. A harmonized model structure should be complex enough to take into account all important physiological processes undergone by any component in an integrated fashion; the same physiological structure must underlie each of the individual models. The initial framework for such a model is developed here on the basis of observed kinetic behavior of nonane, an aliphatic JP-8 component. Its structure is identical to that of decane, shown in Figure 2. A more complete discussion of our harmonized model framework is given in Section 4 below.

Nonane is highly lipophilic and distributes preferentially in brain tissue. Its behavior in the body can be described in a PBPK model that includes the blood, lungs, liver, slowly perfused tissue, rapidly perfused tissue, brain, skin and fat. The model incorporates absorption via inhalation and dermal exposure (broken arrows in Figure 2). It predicts body burdens of nonane under occupational exposure conditions and is consistent with limited occupational body burden data. The implications of this model for modeling jet fuel, in which the components of JP-8 interact via joint metabolic pathways or through mutual effects on tissue distribution, are explored.

A second purpose of the Robinson and Merrill technical report (2008), aside from presenting the model outlined above, was to present data generated by Caracci and others in 1995, which were not previously reported in any public forum. The data include nonane tissue:air partition coefficients, determined by the vial equilibration method, for nonane in blood, liver, fat and brain. Average values and standard deviations reported were: blood:air = 5.22 + 1.26, liver:air = 7.53 + 2.10, fat:air = 1467.42 + 291.53, muscle:air = 6.00 + 2.20, and brain:air = 27.04 + 7.60. Kinetic data are presented from a rat four-hour nose-only inhalation study; blood, liver, muscle and fat nonane concentrations were determined over a time course in rats exposed to 100, 500 and 1000 ppm nonane.

The inclusion of these partition and kinetic time course data in the technical report provides a citable reference for researchers interested in nonane kinetics. In addition, a manuscript based on the modeling work described in the technical report is being prepared.

Discussion of Decane/Nonane Models

Satisfactory simulations of experimental decane and nonane data were achieved using essentially the same model structure for both alkanes. Experimentally-determined partition coefficients were used in both models. Fat kinetics are particularly interesting. Decane predictions suggest a dose-dependent difference in the rate of diffusion into fat. In general, diffusion of decane into these tissues appeared to be slower at 1200 ppm than at 100 ppm, requiring PA_F values of 0.06 and 0.7 mg/hour, respectively. However, no increase in PA_F was required to simulate the end of exposure time point in fat from exposures ranging from 271 to 1200 ppm in the Perleberg data set, suggesting a highly non-linear change in the rate n-decane diffuses into fat. This aforementioned phenomenon has been seen with other lipophilic compounds, such as trichloroethylene (TCE) (Albanese *et al.*, 2002).

A possible physiological basis for this may be anesthetic effects at higher doses. Perleberg did not report on the behavioral effects from decane exposures in rats, but Lof *et al. (*1999) reported anesthetic effects after one week exposure to 800 ppm dearomatized white spirits. During anesthesia, not only is blood flow diverted from non-critical organs, such as fat, but a decrease

in vascularity and/or vascular permeability may occur. Capillary de-recruitment causes a decrease in capillary density and an increase in inter-capillary distances for diffusion, thus reducing the effective diffusion coefficient. Therefore, the possibility of acute high exposures to decane (e.g., 1200 ppm as in Perleberg *et al.*) inducing anesthetic effects, which would result in a lower rate of diffusion into fat than at lower doses, was explored. Satisfactory model predictions of fat at 1200 ppm could be achieved by either reducing fat blood flow from 9 percent to 1 percent of cardiac output or by decreasing the PA_F to 0.06 mg/hour.

Although fat has not been identified as a target tissue for either nonane or decane, the disposition of these chemicals in fat is key to their overall systemic distribution. An adipose model compartment that doesn't accurately capture the uptake of a lipophilic compound can lead to underprediction of the compound's half-life. In addition, current lipidomics research indicates that fat cells are not inert and secrete various hormones and precursors. Hence, fat may actually be an overlooked target tissue, and the importance of fat dosimetrics may be critical to the health of adipocytes.

The overprediction of blood levels at the earliest time-points of the Perleberg data may be physiologically reasonable. Given the high vapor pressure of decane and the fact that tissues were collected 2-3 minutes post-exposure, vapor loss is expected. In addition, Perleberg reported an extraction efficiency from blood of approximately 42 percent indicating that actual blood levels should be higher than measured.

Loss due to alveolar scrubbing was accounted for in the model. Studies on the kinetics of white spirits (which typically are approximately 48 percent straight-chain alkanes, 83 percent total alkanes) have shown that a fair amount is scrubbed by the upper respiratory, until high concentrations are reached and the scrubbing capacity of the upper respiratory tract becomes overwhelmed. Astrand *et al. (*1975) exposed human volunteers to 1250 and 2500 mg/m^3 white spirits for 30 minutes during rest or exercise; during rest, the alveolar air concentration was 25 percent and 15 percent, respectively, of the inspired air concentration and 50 percent and 20 percent during exercise, corresponding to light work. Hence, using a scrubbing factor of 0.7 (an assumption of 30 percent vapor loss to upper respiratory mucous clearance) appears conservative, given that occupationally relevant exposure concentrations are more likely to result in even less penetration to the alveolar region.

Liver metabolism of both alkanes has minimal effect on their kinetics. Existing data indicates slower clearance of these aliphatics in the liver than in blood, suggesting some diffusion limitation in this tissue or possibly intertissue transfer of lipophilics from fat. The decrease in serotonin seen in the dearomatized white spirit study by Lof *et al.* may have implications in the modeling of mixtures effects from chronic exposures. Hypothetically, given serotonin is a potent liver mitogen, a decrease may result in a decrease in liver regeneration and therefore decreased metabolism. Such an effect may alter the competition between multiple hydrocarbon components for metabolism by liver enzymes.

Predictions of n-decane kinetics in blood, fat and brain from exposures to dearomatized white spirits by Lof *et al.* were well within an order magnitude from measured values. Because only the decane content in the white spirit liquid was measured, actual decane content in its vapor is not known. It is likely that the fraction of decane in the actual vapor is higher than its fraction in liquid, given its higher volatility in comparison with the larger branched and cyclic aliphatics in the mixture. In addition, our model predictions may suggest competition with the other white spirit components for partitioning into these tissues. Zahlsen *et al.* (1992, 1993) demonstrated

reduced absorption of alkanes and naphthalenes in comparison with unsaturated hydrocarbons, such as such as alkenes and aromatics.

Predictions of both human blood, fat and expired air predictions were surprisingly close to measured values from exposures to n-decane-containing white-spirit mixtures (Astrand *et al.*, 1975 and Pedersen *et al.*, 1984). Therefore, given these considerations and the satisfactory predictions of n-decane in rat brain, we can assume that the model would provide reasonable predictions of human brain levels, a critical toxicological endpoint.

2. NAPHTHALENE MODEL

Introduction

Naphthalene is the smallest polycyclic aromatic component of JP-8, comprising 0.26 to 1 percent of this fuel (Chao *et al.*, 2005). It has served as a biomarker of dermal and/or inhalation exposure to JP-8 (Dixon and Albers, 2001; Muhammad *et al.*, 2005). The US Air Force is concerned with naphthalene exposures in occupational settings from handling jet fuel and also in environmental settings from fuel spills and contamination. Naphthalene inhalation cancer risk is currently under review by the U.S. Environmental Protection Agency (U.S. EPA). As the U.S. EPA is reviewing the toxicity data for naphthalene and as a stricter cleanup standard will have a significant impact on the U.S. Air Force, 711 HPW/RHPB has assisted the American Petroleum Institute (API) in their effort to conduct research to address data gaps for the reassessment of naphthalene by the U.S. EPA. Through our CRDA with API, we are collaborating with Harvey Clewell to develop a naphthalene PBPK rat model that would address the issues associated with nasal uptake and metabolism. This model, however, does not work in our framework of the n-chem model for jet fuel components (see below). Therefore, the naphthalene model has been harmonized for use in the current project.

Competitive Inhibition

Naphthalene is metabolized by various P450 isozymes in the liver and lung of rats and mice (ATSDR, 2005; Buckpitt *et al.*, 1995; Sweeney *et al.*, 1996) and by P450s in human liver microsomes (Wilson *et al.*, 1996). Some metabolism and toxicity also occur in the nasal passages of the rat (ATSDR, 2005). The specific P450(s) responsible for metabolism in given species, tissues and systems (*in vivo* or *in vitro*) vary, resulting in different ratios of the metabolites, naphthalene-1R,2S-oxide and naphthalene-1S,2R-oxide (Willems *et al.*, 2001). In addition, the availability and depletion of secondary metabolic enzymes (e.g., epoxide hydrolase, GSH) vary with species and tissues. Different abundances and depletion rates of Phase I and Phase II enzymes determine the susceptibility of tissues and result in naphthalene's variable toxicity (Buckpitt *et al.*, 1995; Quick and Shuler, 1999; Willems *et al.*, 2001).

Naphthalene has been shown to be metabolized by multiple P450 isozymes under various conditions (e.g., *in vitro*, *in vivo*, cell types, tissues and species). CYP 2E1, the major P450 responsible for BTEX metabolism (Haddad *et al.*, 1999), in human liver microsomes can metabolize naphthalene *in vitro* (Wilson *et al.*, 1996). Phase I naphthalene metabolism has also been accomplished by CYP 1A1, 1A2, 1B1, 2B4, 2F2, 3A5 and 3A7 (reviewed by ATSDR, 2005). It is important to note, however, that the aryl hydrocarbon regulated P450s (CYP 1A1

and 1A2) metabolize naphthalene *in vitro,* but do not significantly contribute to Phase 1 naphthalene metabolism in mouse studies (Genter *et al.*, 2006). Similarly, the P450 isoform 2B4 exists in the mouse lung and is capable of producing toxic metabolites (Lakritz *et al.*, 1996), but is not important to naphthalene metabolism in that tissue (Buckpitt *et al.*, 1995). Even though non-human primates likely have P450s as their Phase I enzymes, glutathione conjugates are not excreted by rhesus monkeys or chimpanzees, indicating that Phase II metabolism and subsequent toxicity are different from rodents (ATSDR, 2005).

CYP 2F2, a principal P450 in mouse Clara cells, appears to be the main isozyme responsible for the cytotoxicity and genotoxicity in these cells. CYP 2F2 is the Phase 1 metabolic enzyme responsible for the production of naphthalene-1R,2S-oxide. The Phase II metabolites (naphthalene dihydrodiol and glutathione conjugate 2) appear to produce the cytotoxicity and carcinogenicity seen in mouse lungs. The naphthalene-1R,2S-oxide itself does not produce cytoxicity or genotoxicity and the S,R isomer does not further metabolize to toxic compounds (Buckpitt *et al.*, 1995;Quick and Shuler, 1999; Wilson *et al.*, 1996).

In addition to simple competition for metabolism with other JP-8 constituents, naphthalene may also down-regulate P450s when inhaled, redistributing the metabolism of the hydrocarbon to the liver. Repeated exposure to non-lethal concentrations of naphthalene resulted in decreased P450 protein expression levels in the bronchiolar epithelium of mice. The P450 isozyme proteins included CYP 2F2, 2B4 and P450 reductase. All naphthalene glutathione adducts were decreased in these mouse lungs. At the same time, naphthalene exposure resulted in decreased expression of Clara cell secretory protein, an important component of immune-mediated response in the lung. Mice conditioned by prior exposure to 300 ppm of naphthalene for 7 days survived the dose of 500 ppm which was lethal to unexposed control mice (Lakritz *et al.*, 1996).

Additional Aspects of Absorption, Distribution, Metabolism and Elimination

Naphthalene is readily and quickly absorbed via inhalation; occupationally exposed individuals excrete peak levels of metabolites just one hour post-shift. However, naphthalene is only slowly absorbed when ingested as a solid. It was quickly absorbed from a sealed application across shaved rat skin; however, distribution beyond the application site was less than 50 percent of the absorbed dose in 48 hours. In keeping with its lipophilicity, naphthalene was detected in 40 percent of human fat samples and has been found in human breast milk. Naphthalene is also transmitted across the placenta (reviewed by ATSDR, 2005).

Due to a high blood:air partition coefficient and a relatively low vapor pressure, absorbed naphthalene is largely metabolized instead of exhaled (NTP, 2000). Up to 14 percent of the absorbed dose was exhaled from rats exposed dermally (ATSDR, 2005). Metabolism is saturable; metabolic action in the rat lung is saturated more easily than metabolism in the mouse lung. Metabolism in the liver of both species is also saturable, but more comparable. Below metabolic saturation (up to 30 ppm), 65-75 percent of the total inhaled dose was metabolized in 6 hours (NTP, 2000). Excretion is primarily through urine (70-93 percent) while feces accounts for less of the excretion (2-7 percent) (ATSDR, 2005). In the presence of other components of JP-8, it is likely that more competition for metabolism will result in a greater exhaled and excreted proportion of naphthalene.

Existing Naphthalene Models

Because this chemical is of widespread concern, several PBPK models have been developed for naphthalene exposure in rats and mice (Sweeney *et al.*, 1996; Quick and Shuler, 1999; Willems *et al.*, 2001). Each of these models used predicted PC values as the necessary experimental studies have not been performed. Algorithms for predicting PC values may not work well for classes of chemicals different than those on which they were developed (Payne and Kenney, 2002). Experimental rat blood and tissue PC values are desirable for any further naphthalene PBPK modeling efforts. Additionally, time course kinetic data in rat tissues are lacking for naphthalene. The previously published PBPK models have been based on limited blood time course data in rats and mice. Nothing is known about the kinetic behavior of naphthalene in tissues such as liver, fat and muscle.

Five PBPK models currently exist for naphthalene. The Sweeney *et al.* model (1996) was a five compartment flow-limited model for the parent compound, linked via the liver to a five compartment model for naphthalene oxide. Dose routes were intraperitoneal (ip) and oral. The purpose of this model was to track the proportion of the R,S isomer versus the S,R isomer of the oxide and predict the formation of toxic metabolites in the liver and lungs of mice and rats. *In vitro* kinetics parameters were utilized in the model.

Quick and Shuler (1999) were co-authors on the Sweeney *et al.* model and built up their mouse and rat model starting with the previous structure. The five organ compartment models for parent and metabolite now include arterial and venous blood compartments and are linked via both the liver and lung, with Phase I and II metabolism in both organs. Dose routes were ip, intravenous (iv), oral and inhalation. *In vitro* kinetics parameters were utilized.

The National Toxicology Program (NTP, 2000) model was developed to simulate the male and female rat data generated by the NTP the same year. This model consists of five diffusion limited compartments and two blood compartments; only the parent compound kinetics were modeled at this point. Inhalation and iv were the dose routes for the rat study. The modelers used saturable (Michaelis-Menten) kinetics as well as a second saturable metabolic description, the Hill equation, to simulate the data.

The NTP model was formally published by Willems *et al.* (2001). The parent model retained the same structure but was linked to the naphthalene oxide flow limited model from Quick and Shuler (1999) at both the lung and liver. The published version of the model was described by M-M kinetics; the Hill equation was not kept. Depletion and resynthesis of Phase II metabolic enzymes were described and the model was expanded to include mice.

Dixon and Albers (2001) described their model for inhalation and dermal kinetics of naphthalene, as a marker for JP-8, in occupationally exposed humans. Unfortunately their report is an unofficial and nearly unobtainable Air Force compilation. The model structure includes six diffusion-limited compartments, two blood compartments and metabolism in the lungs, liver and skin. Skin and lung metabolism was described by M-M kinetics, while liver was described with a Hill coefficient as well as an M-M equation.

n-Chem: A Continually Updated Interacting Jet Fuel Chemical Model Repository

As PBPK models for jet fuel components are developed (or adapted and harmonized from the literature) and validated, they are integrated into **n-chem,** an *in silico* modeling environment

based in the simulation language ACSL™. At the present time, individual chemical models are linked via competitive metabolic inhibition in the liver, but as we explore more potential interaction mechanisms, these will also be incorporated into *n-chem*. Currently this suite of interacting models includes decane, nonane, benzene, toluene and naphthalene, (see Figure 12 below).
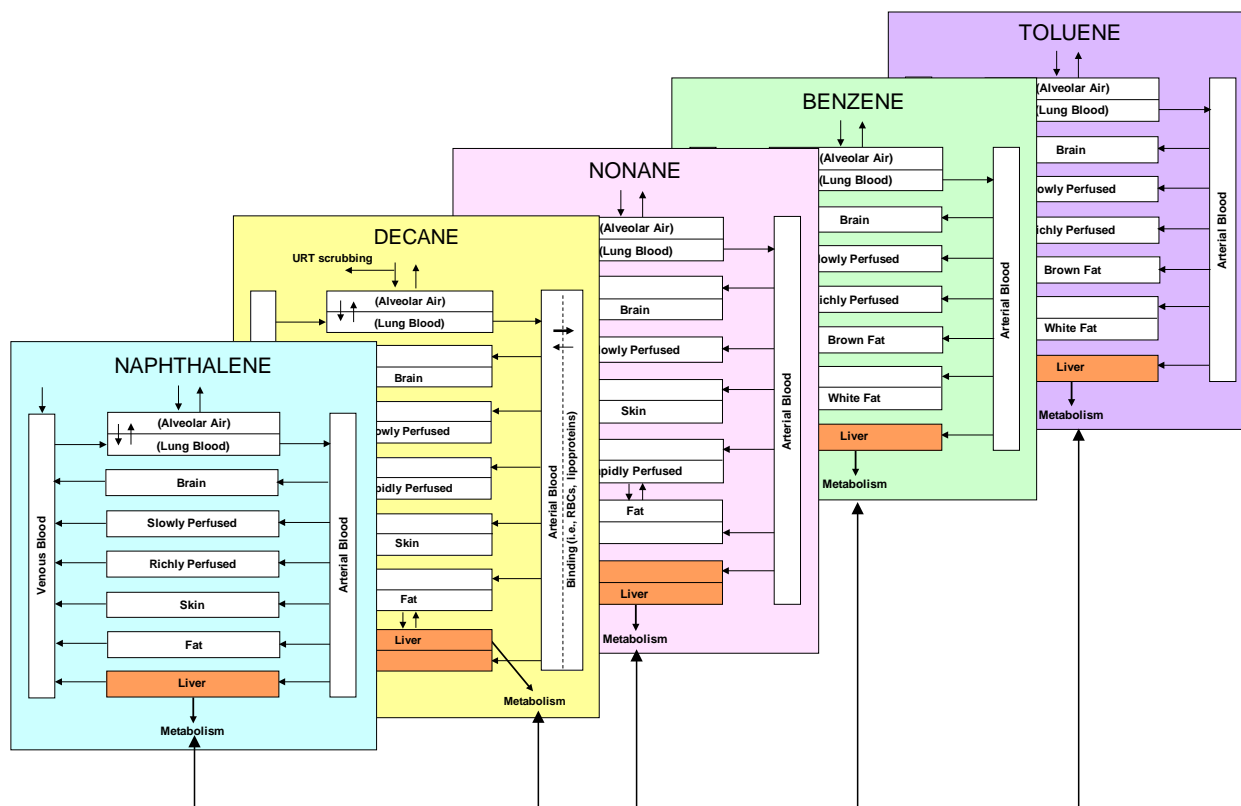
Figure 12. Schematic showing interlinked harmonized suite of PBPK models for JP-8 components currently interlinked via competitive metabolic inhibition

n-Chem Naphthalene Model

A common link between the existing naphthalene models is that all partition coefficients were calculated from published algorithms. Model development for the naphthalene portion of n-chem also began with predicted partition coefficients, particularly those used in the 2000 NTP model and, by attrition, the 2001 Willems *et al.* model. These models utilized PCs calculated and consolidated from algorithms developed by Fiserova-Bergerova *et al. (*1984) and Abraham *et al. (*1985). In turn, Campbell *et al.* used these calculated values in our 2008 SOT abstract and poster on the naphthalene CFD/PBPK model (see Table 6).

Table 6. Partition coefficients used in the naphthalene n-chem model

	Campbell *et al.* *(*2008)	John Morris, UConn (2008, personal communication)	Alan Buckpitt, UCDavis (2008, personal communication)
Method	algorithm[a]	*in vitro*, modified nasal uptake apparatus	*in vitro*, vial equilibration
Species	rat	rat	mouse
PC			
Blood:Air	571.0	544.0	571.0
Brain:Blood[b]	4.0		3.49
Liver:Blood	7.0		1.61
Fat:Blood	106.0		49.0
Slowly Perfused:Blood[c]	4.0		3.49
Richly Perfused:Blood[d]	4.0		2.12

[a] Algorithms developed by Fiserova-Bergerova *et al. (*1984) and Abraham *et al. (*1985); algorithms utilized by and results published by NTP (2000) and Willems *et al. (*2001).
[b] The CFD/PBPK model does not utilize a brain compartment; however the n-chem model requires one (see Figure 2). The brain:air PC for the n-chem model was therefore set equal to the CFD/PBPK model value for "other tissues:blood" (Campbell *et al.*, 2008). When the Buckpitt values became available, the brain:blood PC was again set to the "other tissues:blood" value being used in the CFD/PBPK model.
[c] The slowly perfused:blood PC was set to the muscle:blood PC for each source.
[d] The richly perfused:blood PC was set to the kidney:blood PC for each source.

Of particular importance to the CFD/PBPK model is the blood:air partition coefficient. Due to the significance of this value, John Morris (University of Connecticut, Storrs, CT) measured the rat:blood PC *in vitro*, using a modification to his nasal uptake apparatus (personal communication). The resulting blood:air PC (544) was similar to the PC calculated from an algorithm (571, see Table 6).

Both the CFD/PBPK and the n-chem naphthalene model use only M-M kinetics. Through collaboration with Jerry Campbell (The Hamner Institute, RTP, NC), it was confirmed that just two kinetic data sets exist for rats (intravenous: RTI, 1996; inhalation: NTP, 2000). These data sets only have blood concentrations over time; tissue concentrations were not measured at any time point. Adding the Hill equation or diffusion limitation (using permeability area cross products) is of limited validity without tissue data for comparison. M-M kinetics were found to be sufficient for our purposes, using predicted tissue PCs from Campbell *et al. (*2008) and the experimental blood:air PC from John Morris (see Figures 13 and 14).
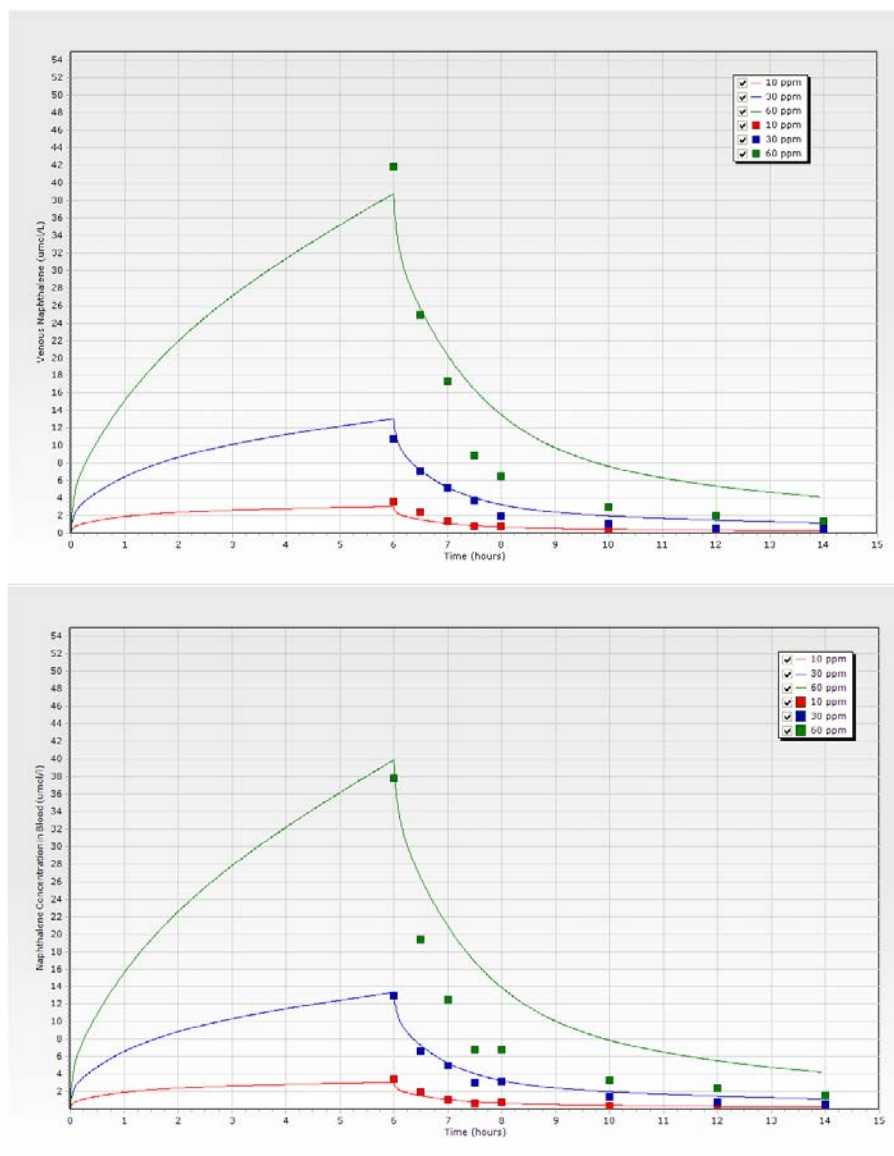
Figure 13. Model predictions of naphthalene in blood (μmol/L) over time (hours) using predicted tissue PCs and the Morris experimental blood:air PC (lines) versus NTP (2000) rat inhalation data (points). Male (top) and female (bottom) rats were exposed for 6 hours to 10, 30 or 60 ppm naphthalene, followed by an 8 hour recovery period.
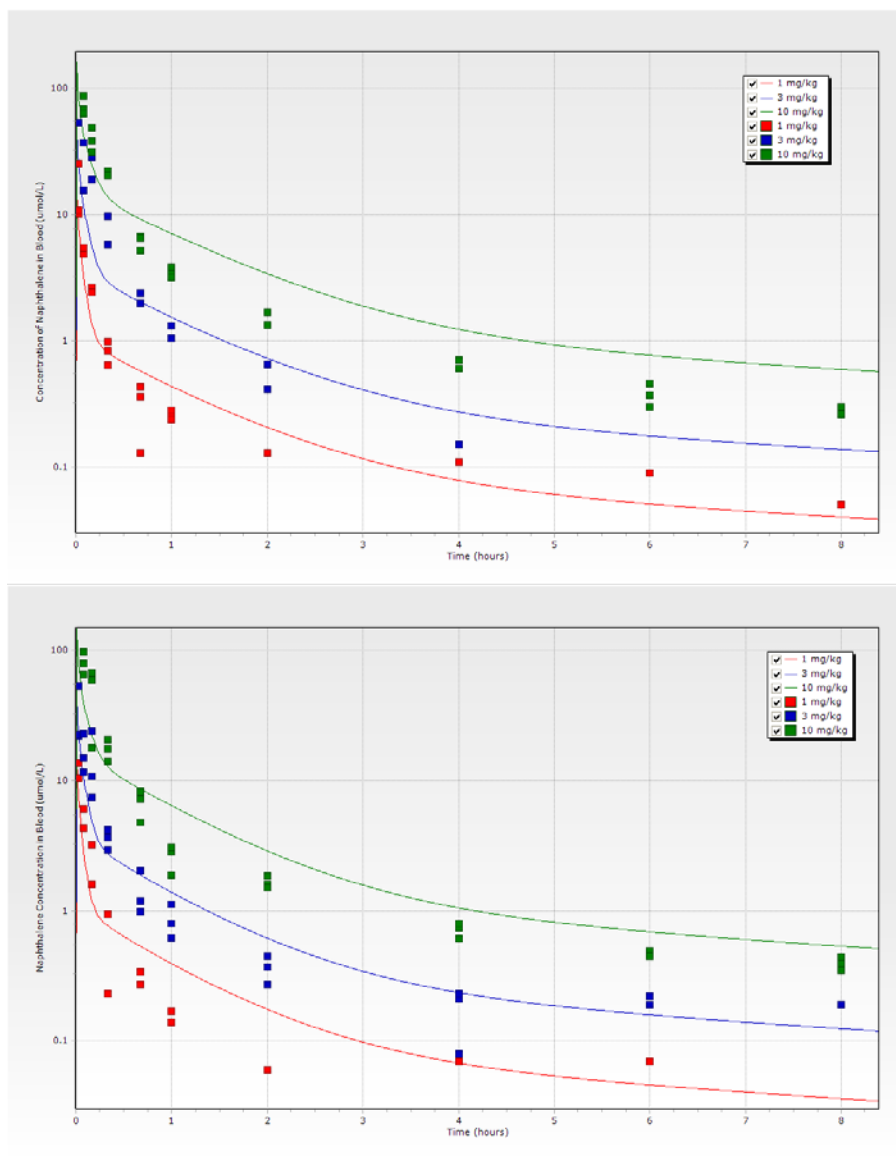
Figure 14. Model predictions of naphthalene in blood (µmol/L) over time (hours) using predicted tissue PCs and the Morris experimental blood:air PC (lines) versus RTI (1996) rat iv data (points). Male (left) and female (right) rats were exposed to 1, 3 or 10 ppm naphthalene intravenously, followed by an 8 hour recovery period.

On 26 June 2008, during the 2008 Naphthalene Research Meeting sponsored by the Naphthalene Research Committee Science Team at the University of Connecticut (Storrs, CT), Alan Buckpitt (UC Davis, CA) indicated that his laboratory had unpublished mouse PCs for naphthalene determined in the 1980s. The tissue:air data were provided in the following weeks (personal communication). The PCs had been determined via an *in vitro* vial equilibration technique. The blood:air PC value (571 ± 76) was identical to the predicted partition coefficient (571), indicating that naphthalene was sufficiently similar to the chemicals for which the original algorithms were developed. However, the resulting tissue:blood values were all lower than those predicted by algorithm. While most differences were not large, Buckpitt's fat:blood PC

was roughly half of the previous predicted value (49 versus 106). Additionally, Buckpitt's liver:blood PC was more than three times lower than the previous value (1.61 vs. 7.0). These lower PCs produced blood concentration predictions that exceed the data concentrations, for all doses except the lowest, with all other model parameters held the same (see Figures 15 and 16).
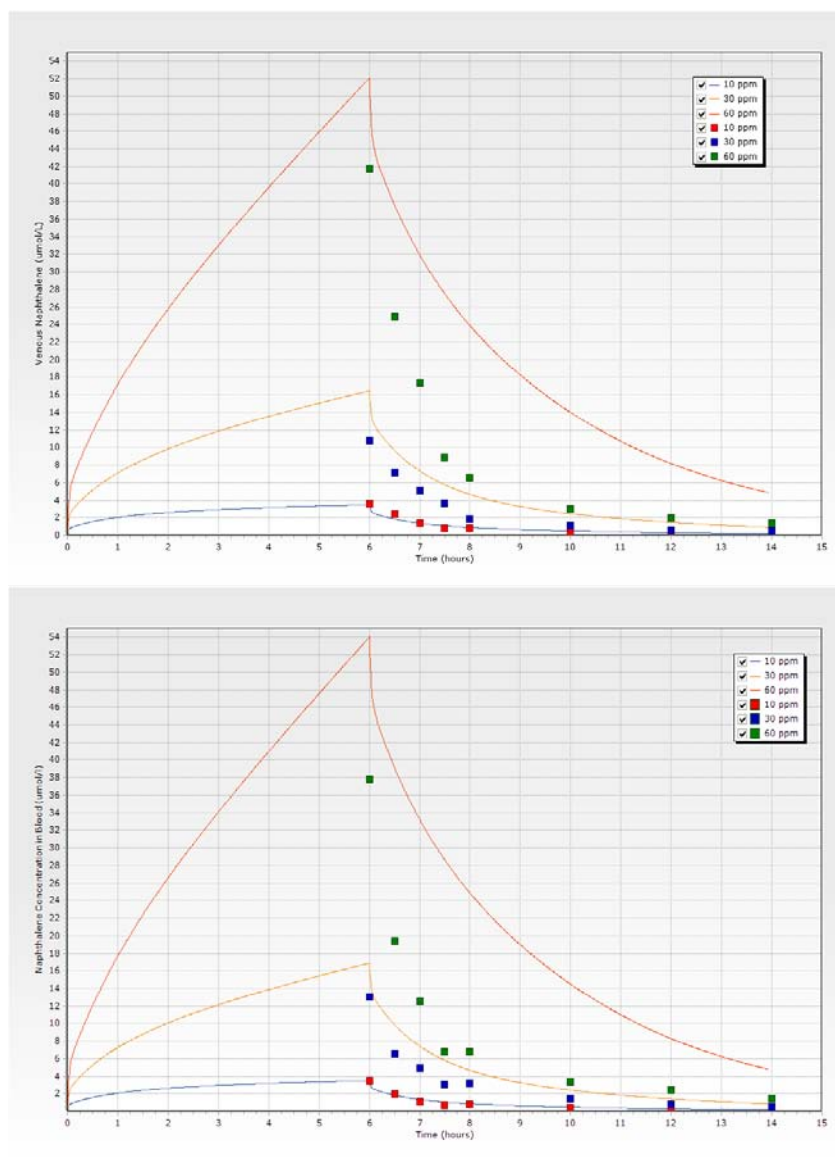
Figure 15. Model predictions of naphthalene in blood (μmol/L) over time (hours) using the Buckpitt experimental PCs (lines) versus NTP (2000) rat inhalation data (points). Male (left) and female (right) rats were exposed for 6 hours to 10, 30 or 60 ppm naphthalene, followed by an 8 hour recovery period.
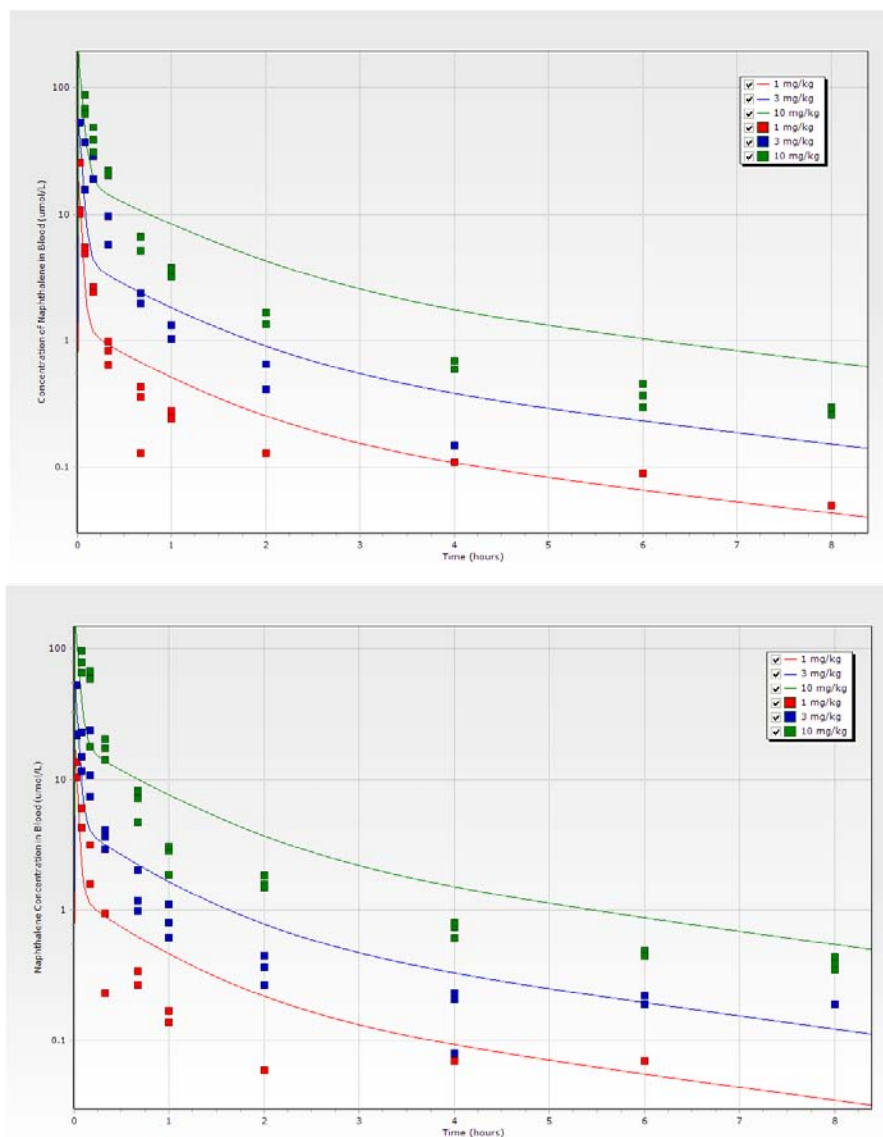
Figure 16. Model predictions of naphthalene in blood (μmol/L) over time (hours) using the Buckpitt experimental PCs (lines) versus RTI (1996) rat iv data (points). Male (left) and female (right) rats were exposed to 1, 3 or 10 ppm naphthalene intravenously, followed by an 8 hour recovery period.

Naphthalene Model Discussion

The n-chem naphthalene model is adequate for predicting the only kinetic data available. The predictions are best using predicted rat tissue partitions, in combination with a measured rat blood:air value. The model does not perform as well using measured mouse partition coefficients. This may be simply a species difference, given that the partitions were measured using mouse blood and tissues and the data being used for simulation comparison are rat blood time courses.

In general, confidence in vial equilibration PCs for naphthalene is not high. In-house attempts have not been successful or reproducible; naphthalene sticks to glassware, as evidenced by partition measurements on glass pieces themselves. Measures to prevent sticking and increase reproducibility have not worked (see Experimental portion of Section 3). Kim *et al. (*2007) reported a very low blood:air PC for human blood (10.3) using vial equilibration. This value doesn't seem credible, given the kinetic behavior observed for naphthalene. Until reproducible and reliable partition coefficients can be determined for naphthalene in blood and tissues, this will remain an area of uncertainty, especially due to the model sensitivity toward the blood:air and fat:blood PCs.

3. COMPLEX MIXTURE MODEL DEVELOPMENT AND EXPERIMENTAL PROGRAM/MODEL VALIDATION

Introduction

We have developed a model of complex mixtures in which interactions are predicted for the competitive metabolic inhibition of a specific enzyme activity (the metabolism component of PBPK modeling) (Robinson, 2001a, b). According to this complex mixture model, the metabolic activity or rate for a single chemical and the complex mixture in which it is a component can be described as if we only had a two component mixture. The total mixture concentration becomes one of the metabolic competitors, and an average value for metabolism is used for its inhibition constant in the model. The purpose of this effort is to validate this mathematical interaction model for JP-8 with experimental animal exposures using a single chemical from the mixture, and JP-8 as the complex mixture, as the two components of the model. Chemical components of JP-8, such as nonane and naphthalene are given to rats individually or in combination with JP-8 using an implanted osmotic pump that delivers a constant rate of chemical over a period of time. A total of 157 male rats will be used resulting in euthanasia by CO_2 overdose after either 6 or 24 hours or 4 days of exposure. Chemical will be measured in blood, urine and tissues (fat, liver, brain and muscle).

Complex Mixture Model

JP-8 components may interact in a number of ways, such as competing for the same metabolic enzymes, or modifying each others' partitioning into various tissues of the body. In order to fully characterize the behavior of any one component, one must simultaneously characterize the effects of all the others. One way to explore these component interactions is to develop PBPK models of individual chemical components and then model these interactions. However, with the large number of components, this becomes an impossibly complex undertaking.

In a recent series of studies, Tardif and colleagues have explored the pharmacokinetic interactions of up to five related compounds, based on the notion that PBPK modeling provides a unique framework that can account for higher order pharmacokinetic interactions based on information from binary mixtures. In particular, they have studied the metabolic interactions between benzene (B), toluene (T), m-xylene (X), ethylbenzene (E) (all components of JP-8) and dichloromethane (D). Analysis of the blood kinetic data suggested that competitive metabolic inhibition of P450 2E1 was the most likely interaction mechanism for these compounds (Tardif *et al.,* 1997; Haddad *et al.,* 1999). CYP2E1 is a member of the cytochrome P450 mixed function oxidase system, involved in the metabolism of xenobiotics, primarily small molecules such as ethanol and benzene. Since JP-

8 is a complex mixture of small hydrocarbon molecules, CYP2E1 is expected to be one of the primary enzymes involved in both the metabolism of JP-8 and competitive metabolic inhibition.

Generalizing the results of Tardif *et al. (*1997) and Haddad *et al. (*1999) to a complex mixture of hydrocarbon components such as JP-8, with competitive metabolic inhibition between each pair of components, the metabolic rate for a particular component *x* in a mixture of an arbitrary number of other components *i* can be written as:

$$RAM_x = \frac{V_{\max}^x c_x}{K_m^x \left(1 + \sum_{i \neq x} \frac{c_i}{K_{ix}}\right) + c_x}$$

where $V_{\max}^x$ is the maximal metabolic rate of *x*, c_x is the concentration of *x*, K_m^x is the (true) Michaelis-Menten constant for *x*, and c_i and K_{ix} are the concentrations and inhibition constants of each component *i*. Rewriting the previous equation gives:

$$RAM_x = \frac{V_{\max}^x c_x}{K_m^x \left(1 + \frac{c_{tot}}{\overline{K}_x}\right) + c_x}$$

where

$$\overline{K}_x = \frac{c_{tot}}{\sum_{i \neq x} \dfrac{c_i}{K_{ix}}} = \frac{1}{\sum_{i \neq x} \dfrac{f_i}{K_{ix}}}$$

is an effective inhibition constant for compound *x* in the presence of other mixture components *i*. c_{tot} is the total concentration of the mixture in the blood (excluding component *x*, which for many complex mixtures may make a negligible contribution to the total) and where f_i is the fraction of the mixture with an inhibition constant K_{ix}.

Note that $\overline{K}_x = 1 \Big/ \sum_{i \neq x} \dfrac{f_i}{K_{ix}}$ is the *harmonic mean* of the individual inhibition constants of the rest of the mixture (weighted according to their relative abundances in the mixture) (Robinson, 2001a, b).

Estimation of metabolism/inhibition kinetic parameters for a majority of the components may need to assume statistical distributions based on incomplete data. For example, for BTEX compounds (Haddad *et al.*, 1999), Ki is distributed (lognormally) with a mean of 0.4 mg/L and a harmonic mean of 0.25 mg/L (see Table 7 and Figure 17). If we assume the same harmonic mean is maintained for the entire JP-8 mixture, we can estimate *RAM_x* for each component of JP-8 in the presence of the others. This prediction can be tested experimentally.

Alternatively, measuring RAMx for a specific component (e.g. nonane, naphthalene), allows $\overline{K}_x$ to be estimated, and the degree of interaction between a particular component and the rest of the fuel to be quantitated.

Note that the degree of interaction is significant only if c_x is not $>> K_m^x$ AND c_{tot} is not $<< \overline{K}_x$ (i.e., if the fraction of x is generally small, but total fuel concentration is relatively high). In general, interaction increases as total fuel concentration increases.

Table 7. Inhibition constants for BTEX components

Values of Inhibition Constants (K_i) Obtained by Fitting of PBTK Model Simulations to Data on Blood Concentrations of Parent Chemicals Observed Following Exposure to Binary Mixtures of Benzene (B) and Toluene (T), Ethylbenzene (E), or *m*-Xylene (X) According to the Hypothesis of Competitive Inhibition

Inhibitor	Substrate	K_i (mg/L)
B	T	0.223
B	E	0.626
B	X	0.226
T	B	0.144
T	E	0.948
T	X	0.357
E	B	0.256
E	T	0.168
E	X	0.505
X	B	0.216
X	T	0.328
X	E	1.667

This table is from Haddad *et al.* (1999).
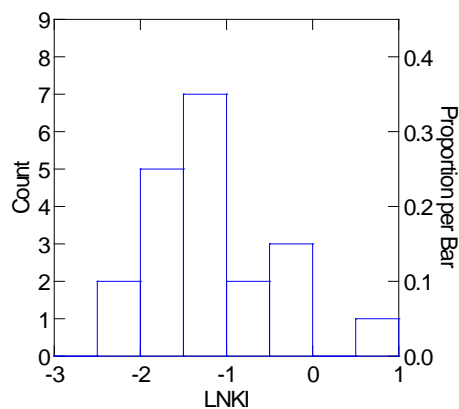
Figure 17. Distribution of logarithms of inhibition constants (Ki) shown in Table 7. This figure is from Haddad *et al.* (1999).

Experimental

Animal Study

The purpose of planning the animal study was to validate the above specific mathematical mixture model for JP-8 in which the components interact via competitive metabolic inhibition of cytochrome P450 2E1 enzyme in the liver. In particular (and in contrast to simple mixtures in which there are just a few components), the total fuel concentration c_{tot} cannot be modeled directly (since it is, of course, a mixture of hundreds of components, each one of which would have to be simulated). It can, however, be either controlled (e.g., kept approximately constant) or measured experimentally. The approach we took in planning the animal study was to measure c_{tot} as the total hydrocarbon content of the blood as estimated by the total area under appropriate GC curves (without identifying individual peaks). We planned to measure RAMx for representative components of jet fuel (nonane and naphthalene) both alone and in the presence of competitors. In order to provide sufficient measurable concentrations of these compounds in tissues, the latter would have been accomplished by spiking these components into the fuel mixture.

The protocol was written and approved to meet the latest DoD guidelines for animal use. The protocol design involved the use of osmotic pumps to deliver JP-8, nonane and naphthalene at steady state doses to male rats over the course of 4 days. Although the animal study was not able to be completed as planned, several preliminary steps were performed to make the study possible in the future.

Osmotic pump compatibility testing

In order to conduct the animal study, compatibility studies between the osmotic pump material and JP-8 and nonane were conducted first using the alzaid® Chemical Comparability Test Kit for ALZET® Osmotic Pumps (DURECT Corporation, Cupertino, CA). The test kit contains polymer spheres that are chemically identical to the polymer used in the reservoir of the ALZET® Osmotic Pumps. According to the results, neither JP-8 nor nonane are compatible with the pump material at concentrations of 17 percent in Volpo saline. We then conducted a second compatibility study for 4 days with 5 percent JP-8 and 5 percent nonane in Volpo saline. Control pumps held only Volpo saline. Although the results were improved by 30 percent for both JP-8 and nonane, 5 percent concentration is still incompatible with the polymer according to the manufacturer's criteria. Next we tested the delivery rate of an osmotic pump *in vitro* with 5 percent JP-8 in Volpo saline at 37°C for one week. Once the pump reached equilibrium it delivered at the expected rate with only a slight decrease on Day 7. Based on these results we decided to proceed with the animal studies.

Pilot Study

A pilot study was then conducted by implanting rats with pumps in a range finding study as well as a determination if osmotic pumps containing the jet fuel or components could deliver adequate amounts of each chemical for up to four days. See Table 8 for an explanation of the number of animals required by dose group. A series of doses were identified that would show the potential interaction between the individual components (nonane and naphthalene) and the entire fuel (JP-8). However, it is not known if the lowest dose (50 mg/kg) can be adequately

detected *in vivo*. That is why for this study a higher dose of 200 mg/kg was used for nonane and naphthalene to ensure a concentration high enough to permit detection. The minimum statistical number of three was sufficient for each dose to be tested in the Pilot Study. For the JP-8, two doses were tested but only one dose will be used in the next experiment. The 750 mg/kg dose is believed to be the appropriate dose for the JP-8 to permit detection of most components of the fuel. However, to deliver this dose, the percent of JP-8 in Volpo saline was 30 percent, which raises even more questions about compatibility of the jet fuel with the osmotic pumps. We also could not find a suitable solvent in which to dissolve the naphthalene. We finally used a 15 percent solution of JP-8 in Volpo saline, which should still show a 50 percent difference in interaction between JP-8 and naphthalene and JP-8 alone. When we tried to make the 200 mg/kg dose of naphthalene in JP-8, the fuel solidified.

Table 8. Animals required for each part of the Pilot Study. Three animals were used for each dose group and were exposed for 4 days via osmotic pumps.

Pilot Study Groups	# of Rats
Control group for analytical sample controls	3
JP-8, 750 mg/kg	3
JP-8, 1000 mg/kg	3
Nonane, 50 mg/kg	3
Nonane, 100 mg/kg	3
Nonane, 200 mg/kg	3
Naphthalene, 50 mg/kg	3
Naphthalene, 100 mg/kg	3
Naphthalene, 200 mg/kg	3
Total	27

Concentrations of naphthalene as low as 125 mg caused the JP-8 to solidify. For the third naphthalene study group, we repeated the 100 mg/kg dose but dissolved it into a fresh solution of JP-8 from the storage drum. For each rat, blood was collected at 12 hours, 2, 3 and 4 days of exposure. Urine and feces were collected 24 and 96 hours after surgery (12 hour collection starting after the 12 hour bleeding) and during the last 24 hours of exposure (day 3 to 4). Tissues were collected on day 4 after removing the rats from the metabolism cages. Liver, fat, muscle and brain were collected after collecting the final blood sample. All samples were frozen and stored until analysis could be performed.

Analytical

In order to measure components of jet fuel in tissue and blood, a sensitive method such as Solid Phase MicroExtraction (SPME) is required. A system was purchased and installed on an existing gas chromatograph (GC). The advantage of SPME is that it is a solvent free technology using a fiber coated with a solid (sorbent) specific to the analyte of interest. The solid fiber coating removes the compounds from the headspace above the sample by adsorption. The fiber is then inserted directly into the GC for desorption and analysis. According to the manufacturer Supelco, SPME has gained wide-spread acceptance as the

technique of preference for many applications including flavors and fragrances, forensics and toxicology, environmental and biological matrices, and product testing.

While we were waiting for the SPME system to arrive and be installed, another animal use protocol was written and approved for *in vitro* determination of partition coefficients (PC) for naphthalene. Method development began for naphthalene PCs using the indirect headspace method (Gargas *et al.*, 1989) with modifications made by Gearhart *et al.* (1993). Preliminary results appeared promising but they were not consistent with existing data or always reproducible. Naphthalene appeared to be sticking to the walls of the sample vials so we tried sialized vials and even measured PC values for large broken pieces of glass vial that we treated as if the glass was tissue. Sialized vials did not prevent naphthalene from sticking and the glass pieces confirmed that glass adsorbs naphthalene. As a result, many times the reference vials with no tissue had counts for naphthalene that were lower than the counts for tissue, resulting in no PC determination as required in the equation below.

$$PC = \frac{(reference\ area\ counts \times vial\ volume) - (test\ area\ counts \times (vial\ volume - sample\ volume))}{(test\ area\ counts \times sample\ volume)}$$

After the SPME was installed, we had software problems for multiple samples in a run as well as limitations based on the GC on which it was installed. We reinstalled the SPME on a newer GC, replaced the computer controlling runs/collecting spectra and updated the analytical software. While conducting method development with the new SPME system, we saw that blood in a glass vial provided more stability and consistency than empty glass reference vials. Partition coefficients were then run for naphthalene by comparing blood in a reference vial with blood and tissue in the tissue vial. Putting blood in both vials actually gave reference counts that allowed the determination of a tissue blood value. This method does not allow you to calculate a blood air value and still had sufficient glass surface exposed that a consistent value could not be obtained whether you measured the naphthalene in the headspace above the blood or in the blood itself. Preliminary data show that completely filling smaller glass reference vials with blood and adding naphthalene could be used to compare to completely filled glass vials with blood and tissue when naphthalene in the blood of both vials is analyzed with the SPME system. Again, no blood to air value is possible but the above equation should produce tissue to blood PC values. Any results obtained by this method will unfortunately not be part of this report and program.

The tissues from the Pilot Study were not analyzed because of analytical issues. Between problems with reinstalling the SPME on a newer GC and upgrading the computer and software and the time and effort to reach the current method for naphthalene PC development, we were unable to attempt to analyze the tissues for JP-8, nonane and naphthalene. Also the longer the tissues were stored, the less reliable the measurements. It is now believed that the incompatibility of the osmotic pumps with the jet fuel, nonane and naphthalene may have resulted in less than optimal delivery of the chemicals even though a flow rate was measured *in vitro* as described above. In order to deliver a solvent using an osmotic pump, an external glass reservoir is needed to hold the chemical while the pump is used to push the chemical out of the reservoir without coming in contact with the chemical. Such an external glass reservoir was finally designed by us and made by a glass blower. We still hope to test this design *in vitro*. If funding is obtained through another source, the modified osmotic pump will be tested *in vivo* and the experimental portion of this program will be completed as a technology transition.

4. HARMONIZED MODEL FRAMEWORK/REPRESENTATIVE COMPOUND SELECTION/MODELING

Harmonized Model Framework: Introduction

Harmonization may be considered to be the imposition of a common model structure for a number of similar but distinct chemicals. The first step in the development of a composite mixture model is to computationally combine two or more "harmonized" single-chemical PBPK models together into a single composite model, in which the chemicals interact in a specific way. For example, Krishnan and co-workers (see, for example, Haddad *et al.*, 1999) have combined PBPK models for BTEX compounds together via their metabolic interaction in the liver (competitive metabolic inhibition of P450-2E1). Such an interaction can in principle be extended to any number *n* of compounds (for which individual single chemical PBPK models are available) that interact via the same pathway, forming a composite simple mixture model ("n-chem" model). It is of course desirable in such a composite model that the underlying single chemical models have the same physiological structure, so that physiological changes, such as, for example, changes in cardiac output or tissue blood flows, will have an overall effect that is readily predictable from parallel effects on the single chemical models. We propose a generic PBPK model structure in which tissues are represented as compartments in which chemicals distribute via the combined effects of diffusion limited uptake from the blood, and diffusion into deep tissue (global tissue model). Both of these processes will not necessarily be needed for all tissues, but they should be available in the generic "harmonized" model structure. Such a model structure also serves as a basis for model refinement and improvement.

Many components of JP-8 are "minor" components, in the sense that they exist individually at very low concentrations, and they are of no particular toxicological concern in themselves. It is not worth developing fully-fledged PBPK models for such compounds, complete with measured blood and tissue partition coefficients, etc. However, it may be useful to have some idea of their kinetic behavior, as a prelude to assessing their potential interactions with components of greater intrinsic concern. For this purpose, a QSAR-based approach for estimating blood and tissue PCs may be useful (Basak *et al.*, 2002). In such an approach, PCs are estimated using information on the chemical's structural properties, together with key biological properties of the tissue itself (Poulin and Krishnan, 1995).

Additional aspects of developing a harmonized model structure for the kinetic behavior of JP-8 components include integration with exposure models of the lung and skin currently being developed in other laboratories. Finally, additional interactions, such as up/down-regulation of metabolic enzymes responsible for the metabolism of other components, and altered partitioning due to chemical interactions in the blood and tissue may also ultimately be needed in a comprehensive composite model structure, although they have not been addressed at this point.

Harmonized Model

For the purpose of the present report, harmonization is considered to be the imposition of a common model structure for a number of similar but distinct chemicals. In this context, two models are harmonized if their model structure is described mathematically in the same way (for example with tissues described with flow limited and/or diffusion limited processes), but with different values for the chemical specific parameters (for partition and/or diffusion coefficients,

for example). Physiological parameters, such as tissue volumes and blood flows, should be the same for all chemicals in a set of harmonized models. In cases in which the behavior of a chemical is sufficiently different from the others that novel processes need to be introduced, a "forced" harmonization may still be possible in which an inclusive model structure is developed, but in which some components "drop out", for example by having certain (chemical specific) parameters set to zero. Such a contingency plan may still allow a harmonized set of models to be developed that would include tetradecane and/or substituted naphthalene if their individual model descriptions turn out to be too different from the existing model structures.

It is envisaged that such a "global" model for lipophilic volatile organics will involve tissue compartments that potentially incorporate both diffusion limited uptake into the tissue together with distribution into a "deep" tissue compartment as follows:

Simple Tissue Model (Flow Limited)

The standard equation describing uptake (partitioning) from blood into tissue (in this case fat) used in the standard Ramsey-Andersen PBPK model is:

$$V_f \frac{dC_f}{dt} = Q_f \left(C_a - \frac{C_f}{P_{fb}} \right)$$

where V_f is the fat volume, C_f is the concentration in fat, assumed to be equilibrated with the venous (outflow) blood concentration C_v via the fat–blood partition coefficient P_{fb}, C_a is the arterial blood concentration, and Q_f is the blood flow to the fat tissue.

Diffusion Limitation into Tissue (Fat)

In some cases, simple partitioning (flow limitation) is not sufficient to characterize uptake into tissues, for example when uptake is restricted (slowed) either by a physical barrier (membrane) or due to the limitation of uptake due to the tissue properties themselves. Such uptake restriction, whatever the cause, is often termed "diffusion-limited uptake". Figure 18 shows axial and radial transport governing mass balance in the fat compartment under these conditions. The equation governing these processes is:

$$V_f \frac{dC_f}{dt} = Q_f \left(C_a - C_v \right) = K \left(C_v - \frac{C_f}{P_{fb}} \right) = \left(\frac{Q_f K}{Q_f + K} \right) \left(C_a - \frac{C_f}{P_{fb}} \right)$$

where K is the "diffusional" transfer coefficient (L/hour) (Andersen *et al.*, 2001).
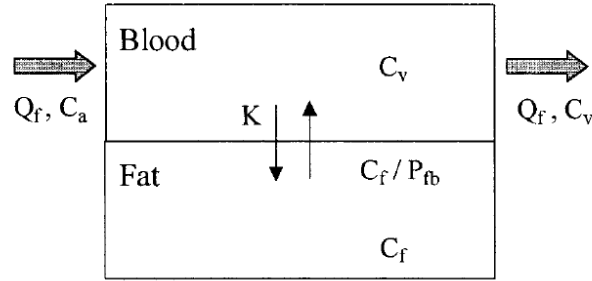
Figure 18. Axial and radial transport governing mass balance in the fat compartment
(from Andersen et al., 2001)

Deep Tissue Compartment

In some cases distribution into a single homogeneous compartment representing the tissue is not sufficient to describe the time-course of uptake. In particular, uptake may better fit a process that involves uptake into a relatively accessible "shallow" compartment from the blood, combined with movement from there into a slower "deep" compartment in the tissue. This may most likely occur in the fat, where yellow or brown fat may be more readily reached from the blood than the very poorly perfused white fat. Figure 19 shows distribution to the deep tissue compartment of an organ. The governing equation in this case is:

$$V_t \frac{dC_t}{dt} = Q_t \left(C_a - \frac{C_t}{P_{tb}} \right) - D_t \left(\frac{C_t}{P_{tb}} - \frac{C_{dt}}{P_{dt:t}} \right)$$

where D_t is the diffusional clearance from tissue t to deep tissue dt, and where, as before, P represents partitioning into these tissues (Andersen *et al.*, 2001).
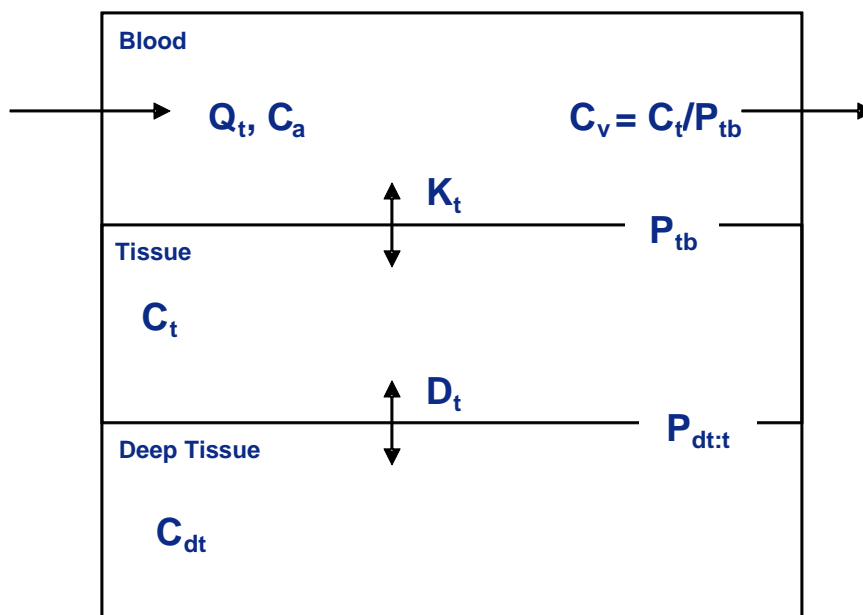
Figure 19. Schematic representation of deep tissue compartment

Combined Diffusion Limitation and Deep Tissue (Global Tissue Model)

Combining both diffusion limitation and movement into a deep tissue compartment gives the following equation:

$$V_t \frac{dC_t}{dt} = \left(\frac{Q_t K_t}{Q_t + K_t} \right) \left(C_a - \frac{C_t}{P_{tb}} \right) - D_t \left(\frac{C_t}{P_{tb}} - \frac{C_{dt}}{P_{dt:t}} \right)$$

Where K_t is the "diffusional" transfer coefficient (L/hour), and D_t is the diffusional clearance from tissue to deep tissue. This is the general form for a generic tissue in a global model, and is the basis for a harmonized framework for highly lipophilic volatile organic compounds such as JP-8 components.

Integration with Exposure Models

Two primary routes of exposure are considered relevant for jet fuel:
- Aerosol/vapor lung deposition
- Dermal absorption

Lung Deposition Model

An aerosol deposition model, such as that of Kleinstreuer and his co-workers, is important to estimate local portal of entry fuel concentrations in the lung for the assessment of potential

immune suppression and irritation effects in the lung. However, for the assessment of the absorbed dose via inhalation to interface with the PBPK models outlined in this report, a simpler assessment of the degree of deposition in the upper respiratory tract (URT), with a focus on what remains for absorption at target sites deeper in the lung, is often sufficient. In this context, consider airflow carrying fuel into the lung at a rate Q (L/hour) (Figure 20).
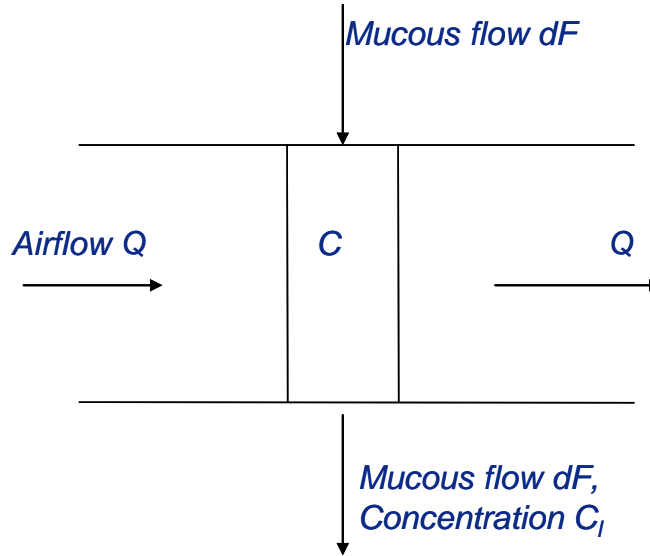
Figure 20. Schematic showing airflow Q through the lung interfacing with an element of mucous flow at some point in the URT. Material carried by the air partitions into the mucous is carried away with total integrated mucous flow F.

The chemical is removed from this small volume element by partitioning into the mucous, and carried away by the mucous flow F (cm³/hour). If the mucous-air partition coefficient is P, then the concentration of agent in the mucous is PC (mol/cm³) and the rate of removal is given by $PCdF$ (moles/hour). By conservation of mass, this equals the difference between the outflow and inflow of agent in the volume element, $-QdC$, so:

$$Qdc = -PCdF \quad or \quad dC/C = -(P/Q)dF$$

Integrating from the input ($C = C_i$) to the output ($C = C_o$) of the URT, for which the total mucous flow is F:

$$\int_{C=C_i}^{C=C_o} \frac{dC}{C} = -\frac{P}{Q}\int_0^F dF$$

or

$$ln(C_i/C_o) = PF/Q$$

The deposition D is then given by:

$$D = 1 - C_o/C_i = 1 - exp(-PF/Q)$$

Note that as partitioning into mucous (P) becomes large, D approaches 1 (complete deposition in the URT). Also, for mucous flow F >> airflow Q, D again approaches 1. On the other hand, or Q >> F, D approaches 0 (no deposition in the URT). Although deposition in the URT means that the chemical is not available for absorption in the deeper regions of the lung (either for local portal of entry effects or systemic absorption), material scrubbed by the mucous will in general be available for absorption via the GI tract.

Dermal Absorption Modeling

In addition to inhalation, dermal absorption is a significant route of exposure, and jet fuel components may be both absorbed systemically and have local skin effects such as irritation (Chao *et al.* 2005). One of the driving factors for skin irritation is the concentration of specific components at specific skin cell types in specific skin layers following dermal exposure to JP-8. In order to quantify these local skin concentrations, a model that incorporates spatial heterogeneity as well as time-dependence, needs to be developed and implemented. Such a model will involve setting up a spatial-temporal framework to represent dermal absorption of chemicals, and developing a partial differential equation (PDE) -based model to monitor the evolution of chemical concentrations in different layers of skin. Such a model will elucidate potential links among exposure-time, concentration, skin depth, and the onset of skin irritation. It is envisaged that such a model will complement the dermal absorption and skin irritation models currently being developed in the laboratories of Dr. McDougal (Wright State University, Dayton, OH) and Dr. Jim Riviere (North Carolina State University, Raleigh, NC).

Surrogate Chemicals

In addition to the representative components of jet fuel already described, it is proposed to develop kinetic models of additional chemicals in the fuel that represent significant fractions of both JP-8 and the new alternative fuels (such as S8 FT fuel). One major class of components that thus far have not been modeled in this context is the branched alkanes. We need to choose a representative compound of this class. Our collaborators at UGA have developed analytical methods to be able to follow a large number of components of both JP-8 and FT fuel in rat tissue and blood (Dietzel *et al.*, 2005). These data will be used to develop an initial model for the chosen compound. The criteria we use to select this compound are the following:
- Abundance in each fuel
- Abundance in blood and tissues, particularly from FT exposure
- Analytical: how easily measured, distinguished from similar compounds, etc.
- Has it been followed in UGA studies to date?
- Potential specific analytical problems (adherence to glass, etc.)
- Is there toxicity information available in the literature?
- Is an authentic standard available for the compound?

Potential candidates for a representative branched alkane are given in Table 9.

Table 9. Potential candidates for a representative branched alkane

RT[a]	Compound[b,c]	CAS	JP-8%	S-8%	List of 53[d]	Tox Info[e]
193.172	4-methylnonane	17301-94-9, 63335-87-5	0.49	1.33		
194.247	**2-methylnonane**	4325-50-2, 871-83-0	0.52	1.43	yes	in vitro, kinetic
195.962	3-ethyloctane[f]	5881-17-4	0.062	0.32	yes	
240.745	**4-methyldecane**	2847-72-5	0.57	1.23	yes	
242.417	**2-methyldecane**	6975-98-0	0.61	1.25	yes	
245.423	**3-methyldecane**	13151-34-3	0.75	1.44	yes	
178.33	3,5-dimethyloctane[g]	15869-93-9	0.043	0.15		
178.63	2,5-dimethyloctane		0.11	0.46		
182.15	2,6-dimethyloctane	2051-30-1	0.44	0.58		
190.44	2,3-dimethyloctane	7146-60-3	0.13	0.27	yes	

[a]RT – retention time on the GC
[b]All isomers of the compounds are listed.
[c]Bolded compound names indicate that authentic standards were used for identification.
[d]List of 53 = one of 53 compounds currently followed in UGA studies
[e]Type of toxicity information existing for the compound; blanks indicate no toxicity information was located
[f]Abundance is fairly low, but has highest abundance for ethyl compound
[g]Dimethyloctanes are less abundant than higher MW dimethyl compounds, but we suspect that these may be more difficult to work with.

Predicting Tissue Partition Coefficients

As PBPK modeling is extended to more components of jet fuel mixtures, key pieces of information are the blood:air and tissue:blood partition coefficients. For more minor components, it will likely prove prohibitive to measure each of these values. Therefore mathematical algorithms predicting tissue and blood partition coefficients (PCs) from solvent properties were compared to assess their usefulness in a petroleum mixture PBPK model (Sterner *et al.*, 2006).

Measured blood:air and tissue:blood PCs for rat and human tissues were sought from literature resources for 14 prevalent jet fuel (JP-8) components. Average experimental PCs were compared with predicted PCs calculated using algorithms from nine published sources. Algorithms chosen used solvent PCs (octanol:water, saline or water:air, oil:air coefficients) due to the relative accessibility of these parameters. Tissue:blood PCs were calculated from ratios of predicted tissue:air and experimental blood:air values (PCEB). Of the 231 calculated values, 27 percent performed within ± 20 percent of the experimental PC values. Physiologically based equations (based on water and lipid components of a tissue type) did not perform as well as empirical equations (derived from linear regression of experimental PC data) and hybrid equations (physiological parameters and empirical factors combined) for the jet fuel components. The major limitation encountered in this analysis was the lack of experimental data for the selected JP-8 constituents. PCEB values were compared with tissue:blood PCs

calculated from ratios of predicted tissue:air and predicted blood:air values (PCPB). Overall, 68 percent of PCEB values had smaller absolute percent errors than PCPB values. If calculated PC values must be used in models, a comparison of experimental and predicted PCs for chemically similar compounds would estimate the expected error level in calculated values (Sterner *et al.*, 2006).

Our method involves the following steps:
- Calculate partitioning into tissue P_t (Poulin and Krishnan, 1995):

$$P_t = (K_{ow} \times F_{nt}) + F_{wt} + (K_{ow} \times 0.3 \times F_{pt}) + (0.7 \times F_{pt})$$

where *F* represents the fraction of tissue weight of a particular component, and subscripts *nt*, neutral lipids in tissue; *wt*, water in tissue; and *pt* phospholipids in tissue. This relation assumes phospholipids comprise 30 percent neutral lipids and 70 percent water.

- Calculate partitioning into erythrocytes P_e and plasma P_p by:

$$P_e = (K_{ow} \times F_{ne}) + F_{we} + (K_{ow} \times 0.3 \times F_{pe}) + (0.7 \times F_{pe})$$
$$P_p = (K_{ow} \times F_{np}) + F_{wp} + (K_{ow} \times 0.3 \times F_{pp}) + (0.7 \times F_{pp})$$

where subscripts are *ne*, neutral lipids in erythrocytes; *np*, neutral lipids in plasma; *we*, water in erythrocytes; *wp*, water in plasma; *pe*, phospholipids in erythrocytes; and *pp*, phospholipids in plasma. This equation makes use of values for the water and lipid content of tissues (Table 10), and of course requires octanol:water partition coefficients (log Kow) for each chemical.

- Finally, calculate tissue-blood partition coefficient by the following equation. We have assumed the hematocrit to be 37 percent.

$$P_{tb} = \frac{P_t}{(0.37 \times P_e) + (0.63 \times P_p)}$$

Table 10: Rat tissue water and lipid composition

Tissue	Water (fraction of tissue weight)	Total lipids (fraction of tissue weight)	Phospholipids (fraction of total lipids)	Neutral lipids (fraction of total lipids)
Blood				
Plasma	0.96	0.0023	0.361	0.639
Erythrocytes	0.63	0.00506	0.77	0.23
Adipose tissue	0.12	0.855	0.0025	0.9975
Liver	0.70	0.06	0.42	0.58
Muscle	0.743	0.019	0.541	0.459

This table is from Poulin and Krishnan (1995).

These and similar methods are also being developed in our laboratory to predict the blood and tissue partitioning of organophosphate compounds.

CONCLUSION

The current project successfully extended the application of traditional physiologically-based modeling (PBPK) techniques to apply to the jet fuel JP-8, a complex mixture of interacting chemical components. Single chemical models of selected representative components (nonane, decane and naphthalene) were developed and used to predict systemic dose for dose-response assessment using kinetic data from in-house and published studies. These models were successfully harmonized by means of a modeling framework that included generic tissue compartments in which we have combined diffusion limitation and deep tissue (global tissue model). A QSAR approach was used to estimate blood and tissue partition coefficients and in integrating our kinetic model with exposure models. A complex mixture model of jet fuel was developed for an arbitrarily large number of components, in which interactions are modeled for the specific case of competitive metabolic inhibition, and experimental techniques for validating such a model were developed. Our computational approach provides a general framework for studying additional mechanisms of interactions between mixture components, as well as other complex mixtures such as alternative fuels. Applications of this approach include the ability to integrate animal, human and *in vitro* data in a form that allows more accurate and reliable internal dose and health effects predictions to be made concerning specific real-world exposures to JP-8 and new alternative fuels.

REFERENCES

Abraham, M. H., Kamlet, M. J., Taft, R. W., Doherty, R. M., and Weathersby, P. K. 1985. Solubility properties in polymers and biological media. 2. The correlation and prediction of the solubilities of nonelectrolytes in biological tissues and fluids. J Med. Chem. 28:865-870.

Albanese, R. A., Banks, H. T., Evans, M. V., and Potter, L. K. 2002. Physiologically based pharmacokinetic models for the transport of trichloroethylene in adipose tissue. Bull. Math. Biol. 64:97-131.

Andersen, M. E., Sarangapani, R., Reitz, R. H., Gallavan, R. H., Dobrev, I. D., and Plotzke, K. P. 2001. Physiological modeling reveals novel pharmacokinetic behavior for inhaled octamethylcyclotetrasiloxane in rats. Toxicol. Sci. 60:214-231.

Astrand, I., Kilbom, A., and P. Ovrum. 1975. Exposure white spirit. I. Concentration of alveolar air and blood during rest and exercise. Scand. J. Environ. Health 1:15-30.

ATSDR. 2005. Toxicological Profile for Naphthalene, 1-Methylnaphthalene and 2-Methylnaphthalene. Agency for Toxic Substances and Disease Registry, Atlanta, GA. http://www.atsdr.cdc.gov/toxpro2.html.

Basak, S. C., Gute, B. D., and Mills, D. 2002. Quantitative molecular similarity analysis (QMSA) methods for property estimation: a comparison of property-based, arbitrary, and tailored similarity spaces. SAR QSAR. Environ. Res. 13:727-742.

Brodde, O. E. 1982. Vascular dopamine receptors: demonstration and characterization by in vitro studies. Life Sci. 31:289-306.

Brown, R. P., Delp, M. D., Lindstedt, S. L., Rhomberg, L. R., and Beliles, R. P. 1997. Physiological parameter values for physiologically based pharmacokinetic models. Toxicol. Ind. Health. 13:407-484.

Buckpitt, A., Chang, A. M., Weir, A., Van, W. L., Duan, X., Philpot, R., and Plopper, C. 1995. Relationship of cytochrome P450 activity to Clara cell cytotoxicity. IV. Metabolism of naphthalene and naphthalene oxide in microdissected airways from mice, rats and hamsters. Mol. Pharmacol. 47:74-81.

Campbell, J. L., Sterner, T. R., Morris, J. B., and Clewell, H. J. 2008. Assessing nasal tissue dosimetry of naphthalene with a hybrid CFD-PBPK model. Toxicol. Sci. 102 (suppl 1):366. (abstract)

Chao, Y. C., Gibson, R. L., and Nylander-French, L. A. 2005. Dermal exposure to jet fuel (JP-8) in US Air Force personnel. Ann. Occup. Hyg. 49:639-645.

Dietzel, K. D., Campbell, J. L., Bartlett, M. G., Witten, M. L., and Fisher, J. W. 2005. Validation of a gas chromatography/mass spectrometry method for the quantification of aerosolized Jet Propellant 8. J. Chromatogr. A. 1093:11-20.

Dixon, K. R. and Albers, E. P. 2001. A model for predicting health risk to exposure to JP8 jet fuel. In: JP8 Final Risk Assessment. R. L. Gibson, ed. Lubbock, TX: The Institute of Environmental and Human Health. pp. 140-151.

Fiserova-Bergerova, V., Tichy, M., and Di Carlo, F. J. 1984. Effects of biosolubility on pulmonary uptake and disposition of gases and vapors of lipophilic chemicals. Drug Metab Rev. 15:1033-1070.

Gargas, M. L., Burgess, R. J., Voisard, D. E., Cason, G. H., and Andersen, M. E. 1989. Partition coefficients of low-molecular-weight volatile chemicals in various liquids and tissues. Toxicol. Appl. Pharmacol. 98:87-99.

Gearhart, J. M., Mahle, D. A., Greene, R. J., Seckel, C. S., Flemming, C. D., Fisher, J. W., and Clewell, H. J., III 1993. Variability of physiologically based pharmacokinetic (PBPK) model parameters and their effects on PBPK model predictions in a risk assessment for perchloroethylene (PCE). Toxicol. Lett. 68:131-144.

Genter, M. B., Marlowe, J., Kevin, K. J., Dragin, N., Puga, A., Dalton, T. P., and Nebert, D. W. 2006. Naphthalene toxicity in mice and aryl hydrocarbon receptor-mediated CYPs. Biochem Biophys Res Commun. 348:120-123.

Gustafson, J. B., Tell, J. G., and Orem, D. 1997. Total Petroleum Hydrocarbon Criteria Working Group Series. Volume 3: Selection of Representative TPH Fractions Based on Fate and Transport Considerations. Amherst, MA: Amherst Scientific Publishers.

Haddad, S., Tardif, R., Charest-Tardif, G., and Krishnan, K. 1999. Physiological modeling of the toxicokinetic interactions in a quaternary mixture of aromatic hydrocarbons. Toxicol. Appl. Pharmacol. 161:249-257.

Kim, D., Andersen, M. E., Chao, Y. C., Egeghy, P. P., Rappaport, S. M., and Nylander-French, L. A. 2007. PBTK modeling demonstrates contribution of dermal and inhalation exposure components to end-exhaled breath concentrations of naphthalene. Environ. Health Perspect. 115:894-901.

Lakritz, J., Chang, A., Weir, A., Nishio, S., Hyde, D., Philpot, R., Buckpitt, A., and Plopper, C. 1996. Cellular and metabolic basis of Clara cell tolerance to multiple doses of cytochrome P450-activated cytotoxicants. I: Bronchiolar epithelial reorganization and expression of cytochrome P450 monooxygenases in mice exposed to multiple doses of naphthalene. J Pharmacol. Exp. Ther. 278:1408-1418.

Lesurtel, M., Graf, R., Aleil, B., Walther, D. J., Tian, Y., Jochum, W., Gachet, C., Bader, M., and Clavien, P. A. 2006. Platelet-derived serotonin mediates liver regeneration. Science. 312:104-107.

Lof, A., Lam, H. R., Gullstrand, E., Ostergaard, G., and Ladefoged, O. 1999. Distribution of dearomatised white spirit in brain, blood, and fat tissue after repeated exposure of rats. Pharmacol. Toxicol. 85:92-97.

Merrill, E. A., Gearhart, J. M., Sterner, T. R., and Robinson, P. J. 2008. Improved predictive model for n-decane kinetics across species, as a component of hydrocarbon mixtures. Inhal. Toxicol. 20:851-863.

Mortensen, B., Eide, I., Zahlsen, K., and Nilsen, O. G. 2000. Prediction of in vivo metabolic clearance of 25 different petroleum hydrocarbons by a rat liver head-space technique. Arch Toxicol. 74:308-312.

Muhammad, F., Monteiro-Riviere, N. A., Baynes, R. E., and Riviere, J. E. 2005. Effect of in vivo jet fuel exposure on subsequent in vitro dermal absorption of individual aromatic and aliphatic hydrocarbon fuel constituents. J. Toxicol. Environ. Health A. 68:719-737.

NTP. 2000. Toxicology and carcinogenesis studies of naphthalene (CAS No. 91-20-3) in F344/N rats (inhalation studies). National Toxicology Program, National Institutes of Health, Research Triangle Park, NC. NTP TR 500.

Payne, M. P. and Kenny, L. C. 2002. Comparison of models for the estimation of biological partition coefficients. J. Toxicol. Environ. Health A. 65:897-931.

Pedersen, L. M., Larsen, K., and Cohr, K. H. 1984. Kinetics of white spirit in human fat and blood during short-term experimental exposure. Acta Pharmacol. Toxicol. (Copenh). 55:308-316.

Perleberg, U. R., Keys, D. A., and Fisher, J. W. 2004. Development of a physiologically based pharmacokinetic model for decane, a constituent of Jet Propellent-8. Inhal. Toxicol. 16:771-783.

Pleil, J. D., Smith, L. B., and Zelnick, S. D. 2000. Personal exposure to JP-8 jet fuel vapors and exhaust at Air Force Bases. Environ. Health Perspect. 108:183-192.

Potter, T. L. and Simmons, K. E. 1998. Total Petroleum Hydrocarbon Criteria Working Group Series. Volume 2: Composition of Petroleum Mixtures. Amherst, MA: Amherst Scientific Publishers.

Poulin, P. and Krishnan, K. 1995. A biologically-based algorithm for predicting human tissue: blood partition coefficients of organic chemicals. Hum. Exp. Toxicol. 14:273-280.

Quick, D. J. and Shuler, M. L. 1999. Use of in vitro data for construction of a physiologically based pharmacokinetic model for naphthalene in rats and mice to probe species differences. Biotechnol. Prog. 15:540-555.

Robinson, P. J. 2000. Pharmacokinetic modeling of JP-8 jet fuel components I. Nonane and C9-C12 aliphatic components. Operational Toxicology Branch, Air Force Research Laboratory, Wright-Patterson AFB. AFRL-HE-WP-TR-2000-0046.

Robinson, P. J. 2001a. Quantifying interactions in complex mixtures such as JP-8 jet fuel. Conference on Application of Technology to Chemical Mixture Research, Fort Collins, CO.

Robinson, P. J. 2001b. Toxicokinetic analysis of complex mixtures: an approach for evaluating exposure to the jet fuel JP-8. Toxicol. Sci. 60(1), 417. (abstract)

Robinson, P. J. 2004. Pharmacokinetic modeling of JP-8 jet fuel components: II. A conceptual framework. Air Force Research Laboratory, Human Effectiveness Directorate, Wright-Patterson AFB, OH. AFRL-HE-WP-TR-2004-0002.

Robinson, P. J. and Merrill, E. A. 2008. A harmonized physiologically-based pharmacokinetic model for nonane as a component of jet fuel. Air Force Research Laboratory, Human Effectiveness Directorate, Wright-Patterson AFB, OH. AFRL-RH-WP-TR-2008-0067.

Robinson, P. J. and Merrill, E. A. Manuscript in preparation. A harmonized physiologically-based pharmacokinetic model for nonane as a component of jet fuel (working title). Preparing for submission to Toxicol. Sci.

RTI. 1996. The toxicokinetics of naphthalene. Protocol RTI-518: The toxicokinetics of intravenously

administered naphthalene (NAP) in male and female B6C3F1 mice and F344 rats. Research Triangle Institute, NTP Chemistry Support Services, RTP, NC. Report S0571.

Smith, A. Q., Campbell, J. L., Keys, D. A., and Fisher, J. W. 2005. Rat tissue and blood partition coefficients for n-alkanes (C8 to C12). Int. J. Toxicol. 24:35-41.

Stanek, K. A., Davis, M. H., Jr., and Coleman, T. G. 1988. Residual effects of ether anesthesia on whole-body hemodynamics and organ blood flows in the rat. J. Pharmacol. Methods. 20:95-102.

Sterner, T. R., Goodyear, C. D., Robinson, P. J., Mattie, D. R., and Burton, G. A. 2006. Analysis of algorithms predicting blood:air and tissue:blood partition coefficients from solvent partition coefficients for prevalent components of JP-8 jet fuel. J Toxicol. Environ. Health A. 69:1441-1479.

Sweeney, L. M., Shuler, M. L., Quick, D. J., and Babish, J. G. 1996. A preliminary physiologically based pharmacokinetic model for naphthalene and naphthalene oxide in mice and rats. Ann. Biomed. Eng. 24:305-320.

Tardif, R., Charest-Tardif, G., Brodeur, J., and Krishnan, K. 1997. Physiologically based pharmacokinetic modeling of a ternary mixture of alkyl benzenes in rats and humans. Toxicol. Appl. Pharmacol. 144:120-134.

Vijayalaxmi, V., Kligerman, A. D., Prihoda, T. J., and Ullrich, S. E. 2006. Micronucleus studies in the peripheral blood and bone marrow of mice treated with jet fuels, JP-8 and Jet-A. Mutat. Res. 608:82-87.

Willems, B. A. T., Melnick, R. L., Kohn, M. C., and Portier, C. J. 2001. A physiologically based pharmacokinetic model for inhalation and intravenous administration of naphthalene in rats and mice. Toxicol. Appl. Pharmacol. 176:81-91.

Wilson, A. S., Davis, C. D., Williams, D. P., Buckpitt, A. R., Pirmohamed, M., and Park, B. K. 1996. Characterisation of the toxic metabolite(s) of naphthalene. Toxicology. 114:233-242.

Zahlsen, K., Eide, I., Nilsen, A. M., and Nilsen, O. G. 1992. Inhalation kinetics of C6 to C10 aliphatic, aromatic and naphthenic hydrocarbons in rat after repeated exposures. Pharmacol. Toxicol. 71:144-149.

Zahlsen, K., Eide, I., Nilsen, A. M., and Nilsen, O. G. 1993. Inhalation kinetics of C8 to C10 1-alkenes and iso-alkanes in the rat after repeated exposures. Pharmacol. Toxicol. 73:163-168.

Zahlsen, K., Nilsen, A. M., Eide, I., and Nilsen, O. G. 1990. Accumulation and distribution of aliphatic (n-nonane), aromatic (1,2,4-trimethylbenzene) and naphthenic (1,2,4-trimethylcyclohexane) hydrocarbons in the rat after repeated inhalation. Pharmacol. Toxicol. 67:436-440.